acidic domain (AhRΔacid; Supplementary Fig. S6a) was indeed unable to promote ER-α ubiquitination *in vivo*, although the mutant retained 3MC-dependent transactivation function (Supplementary Fig. S5c). This indicates that the ubiquitin ligase function of AhR is independent of its transactivation function.

With two separately prepared components of recombinant AhR and CUL4B/DDB1/Rbx1 purified from *Spodoptera frugiperda* (Sf9) cells (Supplementary Fig. S7a), complex assembly *in vitro* was also dependent on 3MC (Fig. 2e). Furthermore, by *in vitro* ubiquitination assay (Supplementary Fig. S7b), the E3 ubiquitin ligase activity of $CUL4B^{AhR}$ for ER-α was dependent on 3MC but not on 17β-oestradiol (E_2) (Fig. 2f). These data indicate that both the complex assembly and the ubiquitin ligase activity of $CUL4B^{AhR}$ may be dependent on AhR agonists.

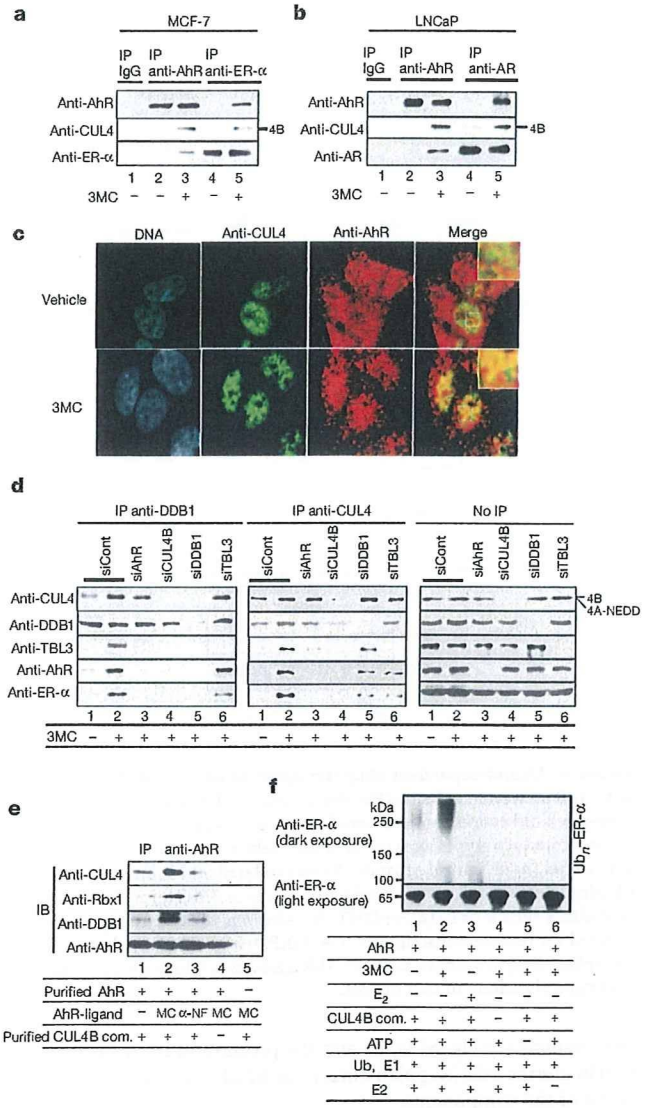

Figure 2 | AhR ligand-dependent assembly and ubiquitin ligase activity of $CUL4B^{AhR}$. **a**, **b**, 3MC-dependent association of endogenous CUL4B and AhR with ER-α and AR. Co-immunoprecipitation analyses from MCF-7 (**a**) and LNCaP (**b**) cells incubated with ligand and MG132 for 2 h. IP, immunoprecipitation. **c**, 3MC-dependent co-localization of AhR with CUL4. MCF-7 cells incubated with 3MC and MG132 for 2 h were immunostained with the indicated antibodies. **d**, Formation of the $CUL4B^{AhR}$ complex. MCF-7 cells were transfected with specified short interfering RNAs (siRNAs) for 48 h, treated with 3MC and MG132 for 2 h, and immunoprecipitated with the indicated antibodies. **e**, Assembly of the CUL4B complex components with AhR is dependent on 3MC *in vitro*. Immunoprecipitation with anti-AhR antibodies of the indicated recombinant CUL4B complex components (CUL4B com.) was observed only in the presence of 3MC. IB, immunoblotting. **f**, $CUL4B^{AhR}$ ubiquitinates ER-α *in vitro*. ER-α protein was incubated with and without recombinant $CUL4B^{AhR}$ E3 complex components, ubiquitin (Ub), ATP, E1 and E2 enzymes as indicated, then subjected to western blotting.

We then examined whether the recognition of sex steroid receptors for 3MC-dependent ubiquitination is indeed mediated by AhR. Co-immunoprecipitation analyses indicated that ligand-activated AhR was required for the recruitment of ER-α (Fig. 2a, d) or AR (Fig. 2b, and data not shown) to $CUL4B^{AhR}$. TBL3 and DDB1 did not seem essential for ER-α recruitment but stabilized the association of ER-α with $CUL4B^{AhR}$ (Fig. 2d). Moreover, knockdown of $CUL4B^{AhR}$ components (Supplementary Fig. S8) impaired the 3MC-induced ubiquitination and degradation of ER-α (Fig. 3a–d, and Supplementary Fig. S9a, b) and AR (Fig. 3e, Supplementary Fig. S9c and data not shown), and abolished the AhR-ligand-induced repression of ER-α transactivation (Supplementary Fig. S10a). Recognition of ER-α by activated AhR was retained, but ubiquitination of AhR-bound ER-α was abrogated, by knockdown of the other $CUL4B^{AhR}$ components (Fig. 3d). An ER-α ΔA/B mutant[15] that lacks interaction with AhR, and an ER-α K7R mutant in which seven lysine residues had been replaced with arginine (Supplementary Fig. S6b), were resistant to AhR-dependent ubiquitination and transrepression (Fig. 3f, and Supplementary Fig. S10b). Taken together, these data suggest that ligand-activated AhR functions as a substrate-specific adaptor component of $CUL4B^{AhR}$. AhR is therefore a unique and atypical substrate-specific component of a cullin-based E3 complex, because AhR bears no known interaction motif with cullin complexes yet associates directly with CUL4B. Ubiquitination of ER-α-associated AhR was similarly abolished by the knockdown, and the overall ubiquitination and degradation of AhR[8,17,18] were partly affected (Supplementary Fig. S11a, b). This implies the existence of $CUL4B^{AhR}$-dependent (self-ubiquitination[3]) and $CUL4B^{AhR}$-independent pathways for AhR degradation.

Human ER-α (hER-α) degradation is reportedly accelerated by the binding of E_2 (ref. 1) or the phosphorylation of Ser 118 (ref. 28), whereas a partial antagonist, tamoxifen, has been shown to stabilize ER-α[1]. Nevertheless, 3MC-activated AhR efficiently induced the ubiquitination and subsequent degradation of tamoxifen-bound ER-α and ER-α-S118A mutant (Fig. 3f). Reciprocally, AhR was dispensable for E_2-dependent ER-α degradation (Supplementary Fig. S11c). These results indicate that the $CUL4B^{AhR}$ system may act independently of innate protein degradation system(s) for ER-α. XAP2/ARA9/AIP[7,8,17], a chaperone that modulates the stability of unliganded AhR, seemed unlikely to mediate the accelerated degradation of ER-α by activated AhR (Supplementary Fig. S11d).

Last, we addressed the physiological significance of $CUL4B^{AhR}$ for sex hormone signalling in intact animals. Injection with either 3MC (Fig. 4a) or β-NF (Fig. 4c) did not affect the expression of ER-α or AR mRNA (data not shown) but caused a decrease in protein levels of uterine ER-α in ovariectomized female wild-type mice and of prostate AR in castrated male wild-type mice (Fig. 4b) regardless of their treatment with cognate sex hormones. However, AhR deficiency ($AhR^{-/-}$ mice)[9,14] abolished such effects of AhR ligands but did not affect the modulation of stability of sex steroid receptors by their respective hormones (Fig. 4a, b). As a result of reduced sex steroid receptor levels after pretreatment with 3MC, E_2-dependent induction of c-*fos* in the uterus[15] and dihydrotestosterone (DHT)-dependent induction of *Probasin* in the prostate[10] were severely impaired (Fig. 4a, b). Cellular proliferation and gene induction in response to sex hormones in primary cultured epithelial cells from normal mouse uterus and prostate were consistently suppressed by 3MC (Supplementary Fig. S12a, b) and β-NF (Supplementary Fig. S12c), but no effect was detected in $AhR^{-/-}$ cells (Supplementary Fig. S12a, b). The significance of $CUL4B^{AhR}$ complex components in the AhR-mediated suppression of sex hormone effects

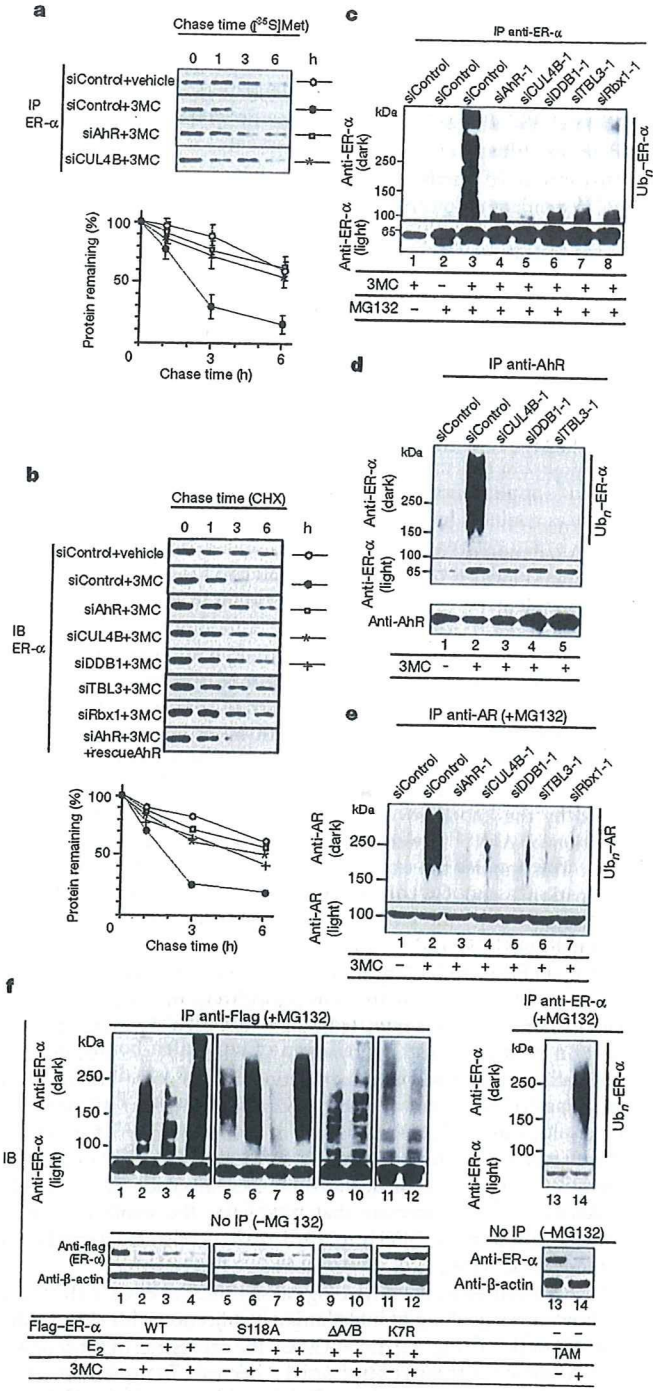

Figure 3 | Activated AhR is a substrate-specific adaptor component of the CUL4B^{AhR} complex. **a–c**, Components of CUL4B^{AhR} are required for 3MC-dependent ubiquitination and degradation of ER-α. MCF-7 cells were transfected with indicated siRNAs for 48 h, then used in pulse-chase analysis as in Supplementary Fig. S3d (**a**), in cycloheximide (CHX) chasing (**b**) and in the *in vivo* ubiquitination assay with ligand incubation for 6 h (**c**). All values are shown as means ± s.d. ($n = 3$) (**a**) or as means ($n = 3$) (**b**). The knockdown efficiency in the same lysates was confirmed in Supplementary Fig. S9a. IB, immunoblotting; IP, immunoprecipitation. **d**, AhR is the substrate-specific adaptor in the targeting of ER-α by CUL4B^{AhR}. MCF-7 cells transfected with the indicated siRNAs were lysed in TNE buffer and immunoprecipitated with anti-AhR antibody in the presence of MG132. Ubiquitination of the ER-α co-immunoprecipitated with AhR was detected by western blotting. **e**, LNCaP cells were subjected to the same analysis as in **a–c**. **f**, AhR-ligand-induced ER-α ubiquitination requires intact lysine residues and is independent of oestrogen binding or S118 phosphorylation of hER-α. Intact MCF-7 cells (right) or cells transfected with Flag–hER-α, AhR and their derivatives (left) were treated with the indicated ligands in the presence (top) or absence (bottom) of MG132 for 6 h, then subjected to western blotting. TAM, tamoxifen; WT, wild type.

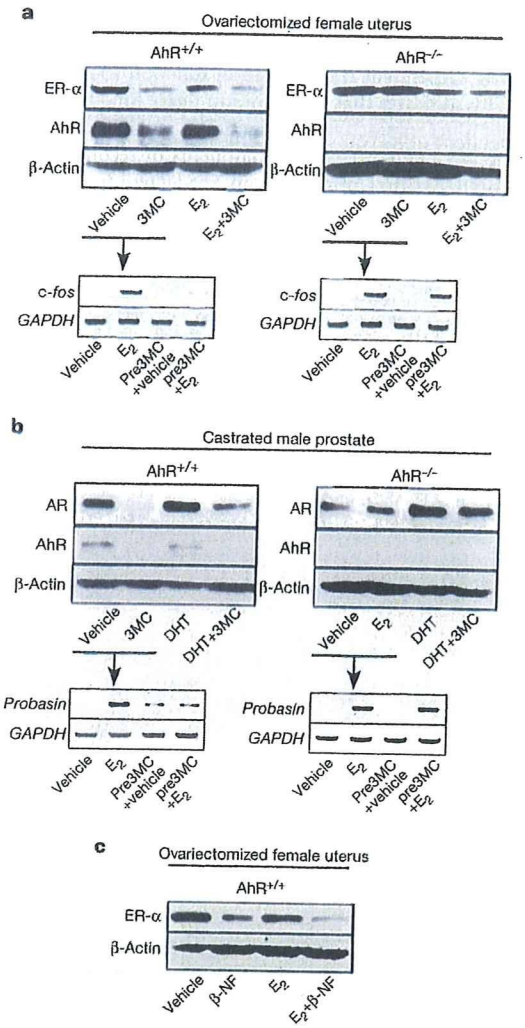

Figure 4 | Ligand-dependent ubiquitin ligase function of AhR *in vivo*. **a, b**, AhR activation enhances the degradation of ER-α and AR *in vivo*. Top: nine-week-old ovariectomized female mice (**a**) or castrated male mice (**b**) of the indicated genotypes were injected with vehicle or indicated ligands. After 4 h, uterus (**a**) or ventral prostate (**b**) was isolated and subjected to western blotting. Bottom: mice pretreated with vehicle or 3MC for 8 h were injected with either vehicle or E_2 (**a**), or DHT (**b**). After 4 h, the uterus or prostate was isolated for reverse transcriptase PCR. GAPDH, glyceraldehyde-3-phosphate dehydrogenase. **c**, Other AhR agonists produce a similar effect on oestrogen signalling to that of 3MC.

(Supplementary Fig. S12a, b) and the promotion of ER-α degradation in uterine cells (Supplementary Fig. S12d) was verified by knockdown of the components.

Here we have shown that a known sequence-specific transcription factor AhR acts as a ligand-dependent CUL4B-based E3 ubiquitin ligase for selectively targeting sex steroid receptors to bring about accelerated protein degradation. The transcription and ubiquitination functions of AhR seem to be responsible for a distinct set of biological events caused by endogenous and exogenous AhR ligands. In ubiquitin ligase complexes, substrate recognition by known

substrate-specific components is generally evoked by substrate modifications[2–4]. However, the recognition and subsequent ubiquitination of sex steroid receptors by AhR requires dioxin-type compounds as ligands but does not require the phosphorylation or ligand binding of sex steroid receptors. We have therefore shown that fat-soluble ligands directly control the function of a ubiquitin ligase complex for targeted protein destruction in animals (see Supplementary Fig. S1). In plants, auxin was recently found to control protein destruction through the auxin receptor SCF^{TIR1} (refs 29, 30). However, whereas SCF^{TIR1} is regulated by ligand-dependent substrate recognition by TIR1, $CUL4B^{AhR}$ is primarily regulated by the assembly of a ligand-dependent complex as well as substrate recognition. Considered together, ubiquitin-ligase-based perception mechanisms of fat-soluble ligands may be diverse in different species. It is possible that other nuclear receptors and binding proteins for fat-soluble ligands also serve as key components of ubiquitin ligases to mediate a non-genomic pathway of fat-soluble ligands to regulate target-protein-selective destruction.

METHODS

More detailed descriptions of all materials and methods are supplied in the Supplementary Information.

Biochemical purification and separation of AhR-associated complexes. The nuclear extracts preparation, anti-Flag affinity purification and mass spectrometry were performed as described previously[15,20]. For purification of the core $CUL4B^{AhR}$ complex, the nuclear extracts were first bound to the GST–CUL4B-N (amino acid residues 1–318) columns before being loaded on anti-Flag columns[20].

***In vitro* ubiquitination assay.** The *in vitro* ubiquitination assay was performed as described previously[23]. Purified Flag–AhR (0.2 μg) was incubated either with 3MC (10 μM) or vehicle (dimethylsulphoxide) for 30 min at 25 °C, then mixed with Flag–CUL4B/DDB1/Rbx1 complex (0.2 μg), and after further incubation for 30 min at 25 °C the substrate, ER-α (Calbiochem), was added.

Plasmids, antibodies, immunoprecipitation, *in vivo* ubiquitination, pulse-chasing, ligand responses in mice, and RNA-mediated interference experiments. Detailed methods used in this study can be found in the Supplementary Information.

Received 13 December 2006; accepted 16 February 2007.

1. McKenna, N. J. & O'Malley, B. W. Combinatorial control of gene expression by nuclear receptors and coregulators. *Cell* 108, 465–474 (2002).
2. Hershko, A. & Ciechanover, A. The ubiquitin system. *Annu. Rev. Biochem.* 67, 425–479 (1998).
3. Deshaies, R. J. SCF and Cullin/Ring H2-based ubiquitin ligases. *Annu. Rev. Cell Dev. Biol.* 15, 435–467 (1999).
4. Harper, J. W. A phosphorylation-driven ubiquitination switch for cell-cycle control. *Trends Cell Biol.* 12, 104–107 (2002).
5. Poellinger, L. Mechanistic aspects—the dioxin (aryl hydrocarbon) receptor. *Food Addit. Contam.* 17, 261–266 (2000).
6. Hankinson, O. The aryl hydrocarbon receptor complex. *Annu. Rev. Pharmacol. Toxicol.* 35, 307–340 (1995).
7. Swanson, H. I. & Bradfield, C. A. The AH-receptor: genetics, structure and function. *Pharmacogenetics* 3, 213–230 (1993).
8. Carlson, D. B. & Perdew, G. H. A dynamic role for the Ah receptor in cell signaling? Insights from a diverse group of Ah receptor interacting proteins. *J. Biochem. Mol. Toxicol.* 16, 317–325 (2002).
9. Mimura, J. & Fujii-Kuriyama, Y. Functional role of AhR in the expression of toxic effects by TCDD. *Biochim. Biophys. Acta* 1619, 263–268 (2003).
10. Lin, T. M. *et al.* Effects of aryl hydrocarbon receptor null mutation and in utero and lactational 2,3,7,8-tetrachlorodibenzo-*p*-dioxin exposure on prostate and seminal vesicle development in C57BL/6 mice. *Toxicol. Sci.* 68, 479–487 (2002).
11. Brunnberg, S. *et al.* The basic helix-loop-helix-PAS protein ARNT functions as a potent coactivator of estrogen receptor-dependent transcription. *Proc. Natl Acad. Sci. USA* 100, 6517–6522 (2003).
12. Matthews, J., Wihlen, B., Thomsen, J. & Gustafsson, J. A. Aryl hydrocarbon receptor-mediated transcription: ligand-dependent recruitment of estrogen receptor α to 2,3,7,8-tetrachlorodibenzo-*p*-dioxin-responsive promoters. *Mol. Cell. Biol.* 25, 5317–5328 (2005).
13. Beischlag, T. V. & Perdew, G. H. ER α-AHR-ARNT protein–protein interactions mediate estradiol-dependent transrepression of dioxin-inducible gene transcription. *J. Biol. Chem.* 280, 21607–21611 (2005).
14. Baba, T. *et al.* Intrinsic function of the aryl hydrocarbon (dioxin) receptor as a key factor in female reproduction. *Mol. Cell. Biol.* 25, 10040–10051 (2005).
15. Ohtake, F. *et al.* Modulation of oestrogen receptor signalling by association with the activated dioxin receptor. *Nature* 423, 545–550 (2003).
16. Romkes, M., Piskorska-Pliszczynska, J. & Safe, S. Effects of 2,3,7,8-tetrachlorodibenzo-*p*-dioxin on hepatic and uterine estrogen receptor levels in rats. *Toxicol. Appl. Pharmacol.* 87, 306–314 (1987).
17. Davarinos, N. A. & Pollenz, R. S. Aryl hydrocarbon receptor imported into the nucleus following ligand binding is rapidly degraded via the cytosplasmic proteasome following nuclear export. *J. Biol. Chem.* 274, 28708–28715 (1999).
18. Roberts, B. J. & Whitelaw, M. L. Degradation of the basic helix-loop-helix/Per-ARNT-Sim homology domain dioxin receptor via the ubiquitin/proteasome pathway. *J. Biol. Chem.* 274, 36351–36356 (1999).
19. Maxwell, P. H. *et al.* The tumour suppressor protein VHL targets hypoxia-inducible factors for oxygen-dependent proteolysis. *Nature* 399, 271–275 (1999).
20. Kitagawa, H. *et al.* The chromatin-remodeling complex WINAC targets a nuclear receptor to promoters and is impaired in Williams syndrome. *Cell* 113, 905–917 (2003).
21. Zhong, W., Feng, H., Santiago, F. E. & Kipreos, E. T. CUL-4 ubiquitin ligase maintains genome stability by restraining DNA-replication licensing. *Nature* 423, 885–889 (2003).
22. Higa, L. A. *et al.* CUL4–DDB1 ubiquitin ligase interacts with multiple WD40-repeat proteins and regulates histone methylation. *Nature Cell Biol.* 8, 1277–1283 (2006).
23. Groisman, R. *et al.* The ubiquitin ligase activity in the DDB2 and CSA complexes is differentially regulated by the COP9 signalosome in response to DNA damage. *Cell* 113, 357–367 (2003).
24. Wertz, I. E. *et al.* Human De-etiolated-1 regulates c-Jun by assembling a CUL4A ubiquitin ligase. *Science* 303, 1371–1374 (2004).
25. Jin, J., Arias, E. E., Chen, J., Harper, J. W. & Walter, J. C. A family of diverse Cul4-Ddb1-interacting proteins includes Cdt2, which is required for S phase destruction of the replication factor Cdt1. *Mol. Cell* 23, 709–721 (2006).
26. Angers, S. *et al.* Molecular architecture and assembly of the DDB1–CUL4A ubiquitin ligase machinery. *Nature* 443, 590–593 (2006).
27. He, Y. J., McCall, C. M., Hu, J., Zeng, Y. & Xiong, Y. DDB1 functions as a linker to recruit receptor WD40 proteins to CUL4–ROC1 ubiquitin ligases. *Genes Dev.* 20, 2949–2954 (2006).
28. Valley, C. C. *et al.* Differential regulation of estrogen-inducible proteolysis and transcription by the estrogen receptor alpha N terminus. *Mol. Cell. Biol.* 25, 5417–5428 (2005).
29. Dharmasiri, N., Dharmasiri, S. & Estelle, M. The F-box protein TIR1 is an auxin receptor. *Nature* 435, 441–445 (2005).
30. Kepinski, S. & Leyser, O. The *Arabidopsis* F-box protein TIR1 is an auxin receptor. *Nature* 435, 446–451 (2005).

Supplementary Information is linked to the online version of the paper at www.nature.com/nature.

Acknowledgements We thank K. Tanaka, C. K. Glass, J. Yanagisawa, Y. Gotoh and J. Mimura for comments; S. Murata, T. Matsuda, T. Suzuki and Y. Tateishi for providing materials; T. Matsumoto, M. Igarashi and S. Fujiyama for technical assistance; and H. Higuchi for manuscript preparation. This work was supported in part by the Program for Promotion of Basic Research Activities for Innovative Biosciences (PROBRAIN) and priority areas from the Ministry of Education, Culture, Sports, Science and Technology (to Y.F.-K. and S.K.).

Author Contributions F.O., T.C., Y.F.-K. and S.K. designed the experiments. F.O., A B., M.O., K I., H.M., S.T. and I. T. performed the experiments. F.O., A.K. and S.K. wrote the paper.

Author Information Reprints and permissions information is available at www.nature.com/reprints. The authors declare no competing financial interests. Correspondence and requests for materials should be addressed to S.K. (uskato@mail.ecc.u-tokyo.ac.jp).

Available online at www.sciencedirect.com
ScienceDirect
ELSEVIER
Biochemical and Biophysical Research Communications 354 (2007) 396–402
BBRC
www.elsevier.com/locate/ybbrc

Identification of amino acid residues in the Ah receptor involved in ligand binding

Kenji Goryo [a], Ai Suzuki [b], Carlos A. Del Carpio [b], Kazuhiro Siizaki [c,1], Eisuke Kuriyama [a], Yoshinori Mikami [a], Koshi Kinoshita [a], Ken-ichi Yasumoto [a], Agneta Rannug [d], Akira Miyamoto [b], Yoshiaki Fujii-Kuriyama [a,2], Kazuhiro Sogawa [a,*]

[a] *Department of Biomolecular Science, Graduate School of Life Sciences, Tohoku University, Sendai 980-8578, Japan*
[b] *Department of Materials Chemistry, Graduate School of Engineering, Tohoku University, Aoba-yama 6-6-11-1302, Sendai 980-8579, Japan*
[c] *Molecular and Cellular Toxicology Section, Environmental Health Sciences Division, National Institute for Environmental Studies, Onogawa, Tsukuba 305-8506, Japan*
[d] *Institute of Environmental Medicine, Karolinska Institutet, SE-171 77 Stockholm, Sweden*

Received 19 December 2006
Available online 10 January 2007

Abstract

The Ah receptor (AhR) is a ligand-activated transcription factor. Five amino acids as candidate amino acids necessary for ligand binding within or near the ligand-binding domain were selected based on their evolutional conservation and their aromatic nature that could interact with xenobiotic ligands. These amino acids were changed to Ala, and the mutated AhRs were subjected to a test of their transactivation activity in HeLa cells. Mutation of Phe318 completely lost its activity whereas other mutations only weakly impaired activity. The Leu-substituted mutant, AhR(Phe318Leu), activated the luciferase activity to the level comparable to wild type in the cells treated with 3-methylcholanthrene (MC) but not at all with β-naphthoflavone (β-NF). Ligand-binding activity of mutants was examined with [^{3}H]MC *in vitro*. AhR(Phe318Ala) could not bind to [^{3}H]MC. [^{3}H]MC bound by AhR(Phe318Leu) was competed with unlabeled MC but not with β-NF. A structural model of the ligand-binding domain was constructed.

Keywords: Ah receptor; Computer modeling; Ligand binding; PAS domain; Xenobiotics

Administration of xenobiotics such as 2,3,7,8-tetrachlorodibenzo-*p*-dioxin (TCDD), 3- methylcholanthrene (MC), and β-naphthoflavone (β-NF) into experimental animals induces several drug-metabolizing enzymes such as CYP1A1 in the liver. These inducers act as ligands for the Ah receptor (AhR), and subsequently, the ligand-activated AhR activates transcription of genes encoding the enzymes [1]. Numerous environmental pollutants, agricultural chemicals, and drugs are known to serve as ligands for the AhR. Polyhalogenated aromatic hydrocarbons such as TCDD and coplanar polychlorinated biphenyls, polycyclic aromatic hydrocarbons such as 3-MC, benzo[a]pyrene and formylindolo[3,2-*b*]carbazoles, and flavonoids such as β-NF are representative potent ligands [1,2]. The most noticeable characteristic of the ligands is that they are organic molecules with planar aromatic rings. In resting cells, the AhR is associated with Hsp90 in the cytoplasm

Abbreviations: AhR, aryl hydrocarbon receptor; MC, 3-methylcholanthrene; β-NF, β-naphthoflavone; TCDD, 2,3,7,8-tetrachlorodibenzo-*p*-dioxin; YFP, yellow fluorescent protein.

* Corresponding author. Fax: +81 22 795 6594.
E-mail address: sogawa@mail.tains.tohoku.ac.jp (K. Sogawa).
[1] Present address: Division of Environmental Genetics, Frontier Science Innovation Centre, Osaka Prefecture University, 1-2 Gakuen-cho, Sakai-city, Osaka 599-8570, Japan.
[2] Present address: Solution Oriented Research for Science and Technology, Japan Science and Technology Corporation, Honchou 4-1-8 Kawaguchi 332-0012, Japan; Department of Molecular and Developmental Biology, Center for Tsukuba Advanced Research Alliance, University of Tsukuba, Tsukuba 305-8577, Japan.

0006-291X/$ - see front matter © 2007 Elsevier Inc. All rights reserved.
doi:10.1016/j.bbrc.2006.12.227

as a soluble receptor. Owing to their lipophilic nature, it is presumed that ligands enter into cells by simple diffusion, and bind to the AhR. Ligand-induced conformation change of the AhR is believed to cause exposure of its nuclear localization signal and succeeding nuclear translocation of the liganded AhR. In the nucleus, the AhR forms a heterodimer with the Ah receptor nuclear translocator (Arnt), and then the heterodimer binds to a specific enhancer termed XRE (DRE or AhRE) localized in the upstream region of target genes [1]. The AhR and Arnt belong to the basic HLH–PAS domain protein family. Vertebrate PAS domains were generally composed of two imperfect repeated regions of about 110 amino acids named PAS-A and PAS-B domains. PAS and HLH domains serve as domains for dimerization with partner PAS proteins. In addition to the dimerization function, some PAS domains contain small organic compounds such as heme, probably for its sensing function [3]. The PAS-B domain of the AhR has the function of binding xenobiotic ligands [4]. The AhR homolog is also distributed in invertebrate species. Interestingly, recent studies demonstrate that *Drosophila* AhR (spineless) and *Caenorhabditis elegans* AhR (AhR-1) have no activity to bind foreign or endogenous chemicals as ligands. Although the protein has no ligand-binding activity, these AhRs heterodimerize with Arnt, binding to the DNA of which sequence is the same as XRE, and activating transcription [5,6].

In this study, we identified amino acids that play a key role in ligand binding of the AhR by several site-directed mutagenesis experiments. Furthermore, a three-dimensional model of the ligand-binding domain was constructed, which demonstrated good agreement with the results of the mutagenesis experiments.

Materials and methods

Construction of plasmids. pBOSFlag-mAhR-HA was constructed as follows. Oligonucleotides, 5′-CCACCGCCCATGGACTACAAAGACG ATGACGATAAAGGCATGGGCTGCA and 5′-GCCCATGCCTTTA TCGTCATCGTCTTTGTAGTCCATGGGCGGTGGAGCT for Flag peptide were inserted into the *Sac*I and *Pst*I site of pBluescript II. Full-length mouse AhR cDNA was inserted into the *Hin*dIII site of the generated plasmid. Using the plasmid as a template, a fragment of Flag-mAhR-HA was generated by PCR using primers, 5′-CCACCGCC CATGGACTACAAAGACGATGACGATAAAGGCATGGGCTGCA (forward) and 5′-CTCGAGCTAGGCGTAGGTCGGGCACGTCGAG GTCGACACACTCTGCACCTTGCTTAGGAATGCC (reverse), and the fragment was inserted into the *Xba*I site of the pEFBOS vector. Expression plasmids for mutated AhRs were produced by site- directed mutagenesis using PCR. Construction of XRE_4-tkLuc was described previously [7]. Chimeric plasmids for pFlag-mAhR-YFP were constructed as follows. A DNA fragment containing the Flag-AhR part of pBOSFlag-mAhR-HA was amplified by PCR, digested by *Bam*HI and *Sal*I and inserted into the *Nhe*I and *Xho*I sites of pEYFPN1 (Clonetech). The resultant plasmid was digested with *Eco*RI and *Bam*HI, treated with Klenow fragment and self-ligated to make the sequence in-frame.

DNA transfection and Western blotting. HeLa cells were grown in MEM supplemented with 10% fetal bovine serum. DNA transfection into Hela cells (grown in a 60 mm dish) was carried out by the calcium phosphate method using 2 μg reporter plasmid XRE_4-tkLuc, 1 μg pBOSFlag-mAhR-HA, 1 μg pBOSmArnt, and 1 μg pBOSLacZ for internal control as described [7]. Western blotting was performed using whole cell extracts from COS-7 cells transfected with pBOSFlag-mAhR-HA or its AhR mutants and a monoclonal anti-HA antibody (Roche, 12CA5). Because of low expression levels of the overexpressed proteins in HeLa cells, HEK293T cells were used to compare the expression levels of various mutants of the AhR, and it was found that they were relatively evenly expressed (data not shown).

Fluorescence observation of cells. CHO-K1 cells were provided by the Cell Resource Center for Biomedical Research, Institute of Development, Aging and Cancer, Tohoku University. Cells grown on the cover glass were transfected with 0.25 μg AhR–YFP fusion plasmids using FuGENE6 transfection reagent (Roche). After incubation for 40 h, cells were treated with MC or β-NF at a given concentration for 2 or 4 h, respectively. Imaging was performed with an Olympus BX50 fluorescence microscope equipped with a filter set (Olympus U-MYFPHQ) and an Olympus DP70 digital camera.

In vitro binding assay. Cytosolic extracts (1 mg protein/ml) from COS-7 cells transfected with expression plasmids for AhRs were prepared as described [8] and [^{3}H]-labeled MC (1 μCi, 1.2 Ci/mmol, Moravek Biochemicals) was added to 450 μl of the extracts. The mixture was incubated at 4 °C for 2 h with or without unlabeled competitors, treated with dextran-coated charcoal and subjected to fractionation by 10–30% (v/v) glycerol gradient centrifugation at 50,000 rpm at 1 °C for 14 h.

Modeling the structure of PAS-B domain. The multiple alignment in the homology modeling procedure was performed based on the predicted and the observed secondary structures of the reference proteins, FixL [9], HERG [10], PHY3 [11,12], EC DOS [13], HIF-2α [14], and PAS kinase [15], while taking into consideration the sequence and structure conservation in their families. A homology model of the mAhR PAS-B domain was generated by means of the modeling module in Insight 2000 (Accelrys Inc.). The docking process was performed using the docking module of the Cerius^2 system (Accelrys Inc.).

Results

Transactivation activity of mutated AhR

Candidate amino acids for ligand recognition and binding were selected on the basis of the following two assumptions. (1) Amino acids are conserved among vertebrate species whose AhRs exhibit ligand-binding activity, but are not conserved in the *Drosophila* and *C. elegans* AhRs that are deficient in binding activity. (2) Interactions between ligands and amino acids include the stacking force between aromatic side chains and aromatic rings of ligands because all ligands have hydrophobic aromatic rings. There were a number of amino acids that satisfied the first criterion. Accordingly, the second criterion was placed on the amino acids. Selection of amino acids satisfying the two criteria revealed five aromatic amino acids within and near the PAS-B domain as shown in Fig. 1A. The amino acids were mutated to Ala, and the transactivation activity of the corresponding mutated AhR was assayed. As shown in Fig. 1B, activity decreased to the basal level in the presence of MC by mutation of Phe318 to Ala. This loss of activity was also seen with other inducers including TCDD and β-NF. Other mutations caused a slight decrease in the transactivation activity. The Phe318 was changed to other amino acids as shown in Fig. 1C, and the transactivation activity of the mutated AhRs was assayed. Substitution to aromatic amino acids, Tyr or Trp, showed an inducible luciferase activity by the stimulus of MC and β-NF,

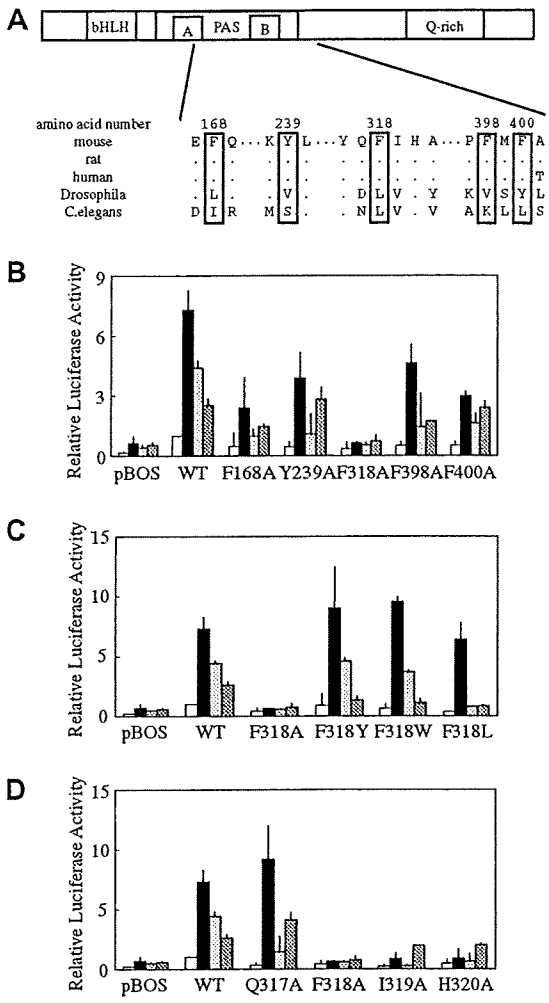

Fig. 1. Transactivation activity of the AhR and its mutants. (A) Alignment of the PAS-B sequences of vertebrate and invertebrate AhR. Structure of the mouse AhR is schematically shown above. Aromatic amino acid residues that were conserved within and around the PAS-B domain of mouse, human, and rat AhRs and that were not conserved in the domain of *Drosophila* and *C. elegans* AhRs were boxed. Dots indicate the same amino acids as those of the mouse AhR. (B) Transactivation activity of the AhRs with mutation of selected amino acids shown in (A). Selected aromatic amino acids were mutated to Ala, and cotransfected into HeLa cells with a reporter plasmid. Four hours after transfection, MC (1 μM), β-NF (0.5 μM), or TCDD (10 nM) were added to the culture medium and cells were further incubated for 40 h. Luciferase activity driven by the AhRs is shown. The values represent means ± SD of at least three separate determinations, and were normalized using the value(s) of wild type AhR treated with DMSO. Open bars, DMSO (vehicle); filled bars, MC; light gray bars, β-NF; dark gray bars, TCDD. (C,D) Transactivation activity of the AhRs with mutations of Phe318 to Ala, Tyr, Trp, and Leu, and transactivation activity of the AhRs with mutation of amino acids neighboring Phe318. Experimental procedures are shown in (B).

probably because the aromatic nature of the side chain was preserved, although induction by TCDD was weak. Mutation to Leu showed a luciferase activity in response to MC with an induction ratio similar to that of wild type, although induced activity was somewhat lower than that of wild type. Interestingly, this mutant exhibited no induction of luciferase activity by the addition of β-NF or TCDD, indicating that this mutation caused a ligand-binding specificity different from the wild type and suggesting that Phe318 may have contact with ligands. Three amino acid residues neighboring Phe318 were changed to Ala. The mutation of Gln317 had no effect on activity although induction by β-NF was weak (Fig. 1D). The mutation of Ile319 or His320 resulted in complete loss of activity, suggesting that these two amino acids also play an important role for ligand binding.

Nuclear translocation of AhRs in response to inducers

Chimeric proteins of mutated AhRs fused to YFP were expressed in CHO-K1 cells, and subcellular localization of the chimeric proteins was observed. These chimeric proteins were evenly expressed and showed transactivation activity similar to the AhR without YFP tag (data not shown). Fluorescence from the YFP moiety of the wild-type AhR fusion protein was diffused over the cell, and treatment of cells with MC caused accumulation of the signal in the nucleus as shown in Fig. 2. Approximately 50% of the fluorescent cells showed nuclear localization at the maximal concentration of MC. The nuclear accumulation was accomplished within 2 h and dependent on the concentration of MC. Nuclear translocation was also observed by the addition of β-NF, although the rate of the translocation was slow, and 4 h was required for completion. The reason is not clear as to why nuclear localization of expressed AhR–YFP did not occur in all fluorescent cells even at high concentrations of inducers. Nuclear localization of mutant AhR(Phe318Ala) was similarly examined. When neither MC nor β-NF was added, nuclear accumulation of the mutant did not occur. Mutant AhR(Phe318Leu) was translocated into the nucleus by the addition of MC similar to the level of the wild type. However, the mutant remained in the cytosol with the addition of β-NF, in accordance with the result of transactivation activity of the mutant. Taken together, these results strongly suggest that stimulus-dependent nuclear localization of mutated AhRs is the causal event for their transactivation activity.

Ligand-binding activity of mutated AhRs

In vitro binding activity of mutated AhRs to [^{3}H]-labeled MC was examined using cytosolic extracts of COS-7 cells transfected with expression plasmids for the AhRs. A clear peak at around the 9S position of the [^{3}H]MC-AhR complex appeared in the glycerol gradient as shown in Fig. 3A. This binding of the radioactive ligand was competed out with 22 times the molar excess of unlabeled MC or β-NF. A similar binding signal was also observed when cytosol containing AhR(Phe318Leu) was used. This signal was competed with unlabeled MC. However, unlabeled β-NF could not compete with the [^{3}H]MC bound to the mutated AhR, reflecting the results of transactivation and

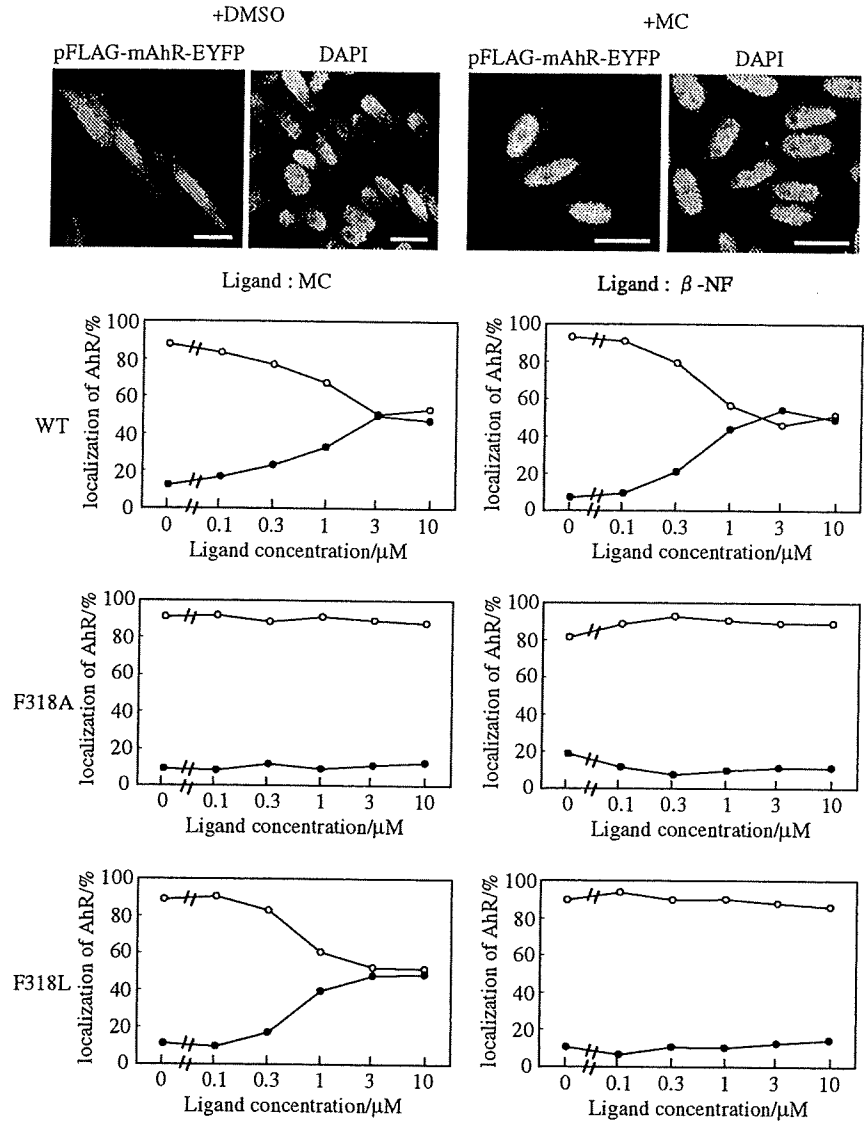

Fig. 2. Nuclear translocation of the AhR and its mutants. CHO-K1 cells were transfected with AhR–YFP-fusion plasmids, and treated with inducers for 2 h (MC) or 4 h (β-NF) before fixation in 4% paraformaldehyde. The fixed cells were counterstained with DAPI. Typical images of fluorescent cells after treatment with DMSO (vehicle) and MC are shown above. Scale bars, 20 μm. Approximately 300 cells were randomly selected, and percentages of cells with only nuclear localization (shown by closed circles) and cells with both nuclear and cytosolic localization (shown by open circles) of the chimeric protein are shown.

nuclear translocation experiments. When cytosol fraction containing expressed AhR(Phe318Ala) was used, no signal of ligand binding was detected. The mutated AhRs were evenly expressed in COS-7 cells as shown in Fig. 3B.

Modeling the AhR ligand-binding domain

Since the three-dimensional (3D) structure of AhR has not been elucidated so far, and previously reported 3D models of the ligand-binding domain have failed to identify Phe318 as a ligand-recognition amino acid [16], we concentrated on the active site of AhR, and obtained a 3D model for it using comparative modeling techniques. A combined FASTA and PSI-BLAST search of the protein data bank (PDB) [17] reveals a high number of matches between mouse AhR PAS-B and other PAS proteins, including HLF (HIF-2α), several histidine kinases, and other light receptors as well as sensor proteins (oxygen/redox sensors) and ion channels (data not shown). Sequences such as HLF, PHY3, HERG, FixL, EC Dos, and PAS kinase were found that were based on a moderate sequence similarity, characterized by E values of less than 10^{-3}. Fig. 4A illustrates the multiple sequence alignment of AhR PAS-B with these sequences. A further alignment of the secondary structure predicted for AhR PAS-B and the secondary structures for the 3D structures extracted from PDB

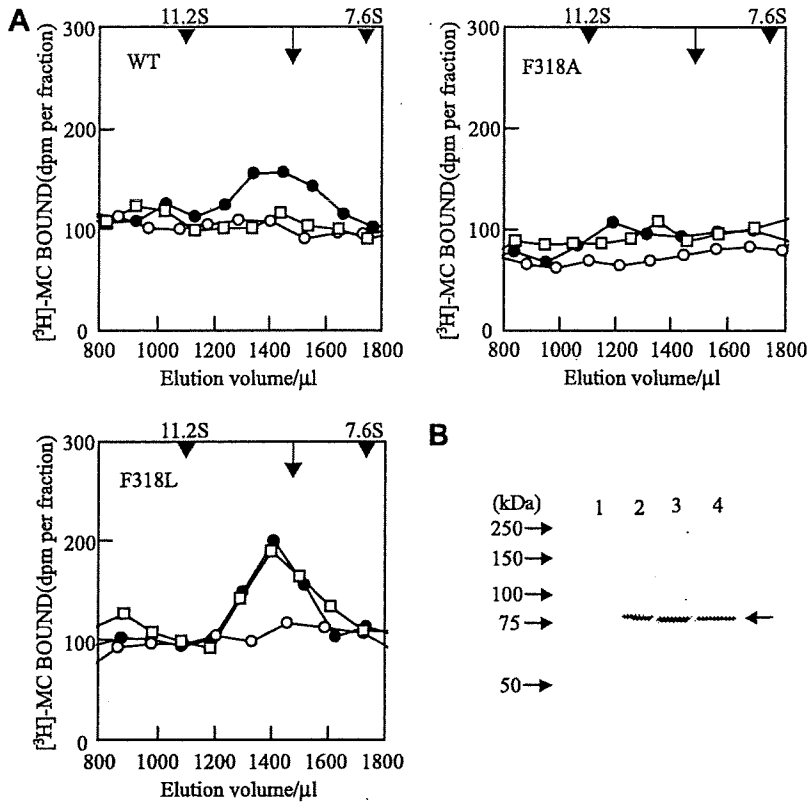

Fig. 3. Ligand-binding activity of the AhR and its mutants. (A) Binding of mutant AhRs to [^{3}H]-labeled MC. AhRs were expressed in COS-7 cells and cytosolic extracts were prepared. Glycerol gradient centrifugation was performed as described under Materials and methods. Fractions (about 100 μl) were collected and radioactivity was counted on a liquid scintillation counter. Catalase (11.2S) and fibrinogen (7.6S) were used as size markers. Arrows show the position of 9S. Filled circle, [^{3}H]MC with DMSO; open circle, [^{3}H]MC with unlabeled MC; open square, [^{3}H]MC with unlabeled β-NF. (B) Expression of mutant AhRs. Western blotting analysis using 20 μg of cell extracts was performed by the ECL plus Western blotting detection system kit. Lane 1, whole cell extracts without transfection; lanes 2–4, cytosolic extracts of cells transfected with expression plasmid for AhR, AhR(Phe318Ala), and AhR(Phe318Leu), respectively. An arrow shows the bands of the AhR.

indicate that the fold of HLF is the optimal template on which to model AhR PAS-B (Fig. 4B). The threading process of the AhR sequence into the template was performed using Swiss PDB viewer (spdbv) software. The structure was further minimized using the GROMOS force field embedded in spdbv to optimize the position of the lateral chains of the amino acids constituting the receptor.

Assisted by the docking module in Cerius^2, we first mapped plausible ligand-binding pockets for the model of AhR PAS-B. A unique deep cavity was recognized by the system, the boundaries of which are constituted by the amino acids in Table 1. The model was then used to dock three ligand molecules, MC, β-NF, and TCDD. The docking process was also performed using the Cerius^2 software. Orientations for the ligands within the binding pocket ranked as the highest by the docking software were further minimized so as to obtain reliable 3D structures for the receptor–ligand complexes. Amino acids in contact with the ligand are identified by computing the fraction of SASA (solvent accessible surface area) buried by each of the amino acids on the ligand. We performed this calculation for β-NF, and Table 1 illustrates the decrement in SASA of β-NF when docked to the cavity of the model of AhR by each of the amino acids composing the cavity. The SASA is computed using Richards' algorithm [18], and a radius for the solvent molecule (water) of 1.4 Å. The buried SASA is calculated as the difference of the SASA of β-NF at the isolated state minus the SASA of β-NF when it is in contact with each of the amino acids listed in Table 1. Docking models of the complex of AhR with TCDD, MC or β-NF, show their extensive contact with Phe318, Ile319, and His320 (Fig. 4C). Extensive hydrophobic interaction can also be observed with Ala328, Met342, Leu347, and Leu348. Two lysine residues (Lys284 and Lys286) suggest the formation of hydrogen bonds with the oxygens on the aromatic rings of β-NF.

Discussion

From the results shown in Fig. 1, it is suggested that Phe318 plays a critical role in ligand binding to AhR. The importance of this amino acid is also demonstrated by the complex model of AhR PAS-B that we built by comparative modeling and docking simulations. The decrement

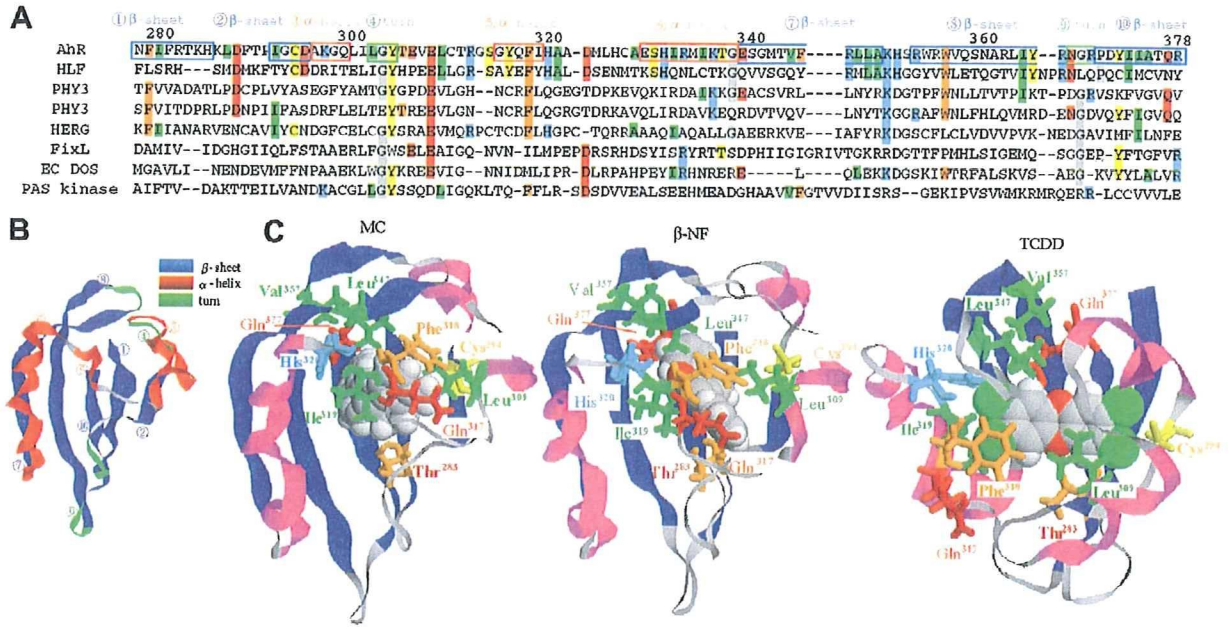

Fig. 4. Model of the AhR PAS-B domain and contacts between ligands and amino acid residues in the binding pocket. (A) Sequence alignment of AhR-related sequences. Sequences of Mouse AhR, human HLF (HIF-2α), PHY3 from *Chlamydomonas reinhardtii* (upper sequence) and *Adiantum capillus-veneris* (lower sequence), human HERG, *Bradyrhizobium japonicus* FixL, *Escherichia coli* EC DOS and human PAS kinase were aligned. Secondary structure regions are shown above the sequences. (B) Ribbon-style drawing of the AhR PAS-B domain. Numbers show the secondary structure regions as shown in (A). (C) Model of MC, β-NF, and TCDD in the binding site of AhR PAS-B domain. Secondary structure elements are colored blue (strands) and red (helices).

Table 1
Calculated buried SASA of β-NF by amino acids in the binding region of AhR

Amino acid	Difference in SASA (in Å^2) for β-NF
THR283	0.07
LYS284	73.37
LYS286	49.73
CYS294	0.07
GLN299	72.54
GLY303	47.77
TYR304	29.22
LEU309	0.07
CYS310	27.07
GLY315	46.93
GLN317	0.07
PHE318	84.37
ILE319	77.81
HIS320	60.62
ALA328	81.26
SER330	43.35
MET342	73.18
LEU347	88.59
LEU348	87.90
ALA349	42.20
VAL357	37.66
SER359	61.20
ALA375	0.00
GLN377	41.40

in the SASA of β-NF due to contact with Phe318 is large (about 84 Å^2, Table 1), suggesting that extensive interaction exists between the residue and the ligand. Mutation of Phe318 by Leu completely eliminated responsiveness of the mutant towards β-NF, although responsiveness to MC remained unchanged. Binding experiments using [^{3}H]MC corroborate the geometry of our modeled complex, since the location of Phe318 at the ligand-binding surface of the receptor plays a key role in ligand-binding specificity. This is clearly shown by the mutations performed on Phe318 that caused changes in the binding activity of the receptor. Moreover, two amino acids, Ile319 and His320, neighboring Phe318, were both found to play an essential role in the binding activity of the receptor. Although contact surface areas of these amino acids with the docked ligands are less than that of Phe318, their relevance in the binding affinity of the receptor cannot be neglected. In fact, Ile319 has been reported to be important in avian AhRs [19]. The Ile residue (Ile324 corresponding to Ile319 in the mouse AhR) of the chicken AhR that showed high affinity towards TCDD was changed to Val in tern AhR that exhibited low TCDD-binding activity. As shown in Fig. 1D, a large decrement in the activity of the receptor was observed when they were mutated to Ala. Therefore, the importance of these two amino acids in the binding of the ligands can be rationalized in terms of their bulky lateral chains and polar characteristics. The imidazole group in His confers it a polar property absent in Ala while Ile has a larger chain and is more strongly hydrophobic. Thus, mutations of these amino acids have strong repercussions in the activity of the receptor. Ala375, whose allelic mutation was demonstrated to be

responsible for the different ligand-binding affinity between C57BL/6 and DBA/2 mouse strains [8] was also exposed into the ligand-binding pocket, although it does not appear to be in direct contact with β-NF in the model. Further mutagenesis studies are necessary to confirm the amino acids composing ligand-binding domain of the AhR.

Acknowledgments

This work was supported in part by Grant-in-Aid for research from the Ministry of Education, Culture, Sports, Science and Technology of Japan, and by funds for Research for the Future Program of JSPS.

References

[1] J. Mimura, Y. Fujii-Kuriyama, Molecular mechanisms of AhR functions in the regulation of cytochrome P450 genes, Biochem. Biophys. Res. Commun. 338 (2005) 311–317.

[2] L. Bergander, N. Wahlstrom, T. Alsberg, J. Bergman, A. Rannug, U. Rannug, Characterization of in vitro metabolites of the aryl hydrocarbon receptor ligand 6-formylindolo[3,2-*b*]carbazole by liquid chromatography-mass spectrometry and NMR, Drug Metab. Dispos. 31 (2003) 233–241.

[3] E.M. Dioum, J. Rutter, J.R. Tuckerman, G. Gonzalez, M.A. Gilles-Gonzalez, S.L. Mcknight, NPAS2: a gas-responsive transcription factor, Science 298 (2002) 2385–2387.

[4] K.M. Dolwick, H.I. Swanson, C.A. Bradfield, In vitro analysis of Ah receptor domains involved in ligand-activated DNA recognition, Proc. Natl. Acad. Sci. USA 90 (1993) 8566–8570.

[5] J.A. Powell-Coffman, C.A. Bradfield, W.B. Wood, *Caenorhabditis elegans* orthologs of the aryl hydrocarbon receptor and its heterodimerization partner the aryl hydrocarbon receptor nuclear translocator, Proc. Natl. Acad. Sci. USA 95 (1998) 2844–2849.

[6] R.B. Emmons, D. Duncan, P.A. Estes, P. Kiefel, J.T. Mosher, M. Sonnenfeld, M.P. Ward, I. Duncan, S.T. Crews, The spineless-aristapedia and tango bHLH-PAS proteins interact to control antennal and tarsal development in *Drosophila*, Development 126 (1999) 3937–3945.

[7] J. Mimura, M. Ema, K. Sogawa, Y. Fujii-Kuriyama, Identification of a novel mechanism of regulation of Ah (dioxin) receptor function, Genes Dev. 13 (1999) 20–25.

[8] M. Ema, N. Ohe, M. Suzuki, J. Mimura, K. Sogawa, S. Ikawa, Y. Fujii-Kuriyama, Dioxin binding activities of polymorphic forms of mouse and human arylhydrocarbon receptors, J. Biol. Chem. 269 (1994) 27337–27343.

[9] W. Gong, B. Hao, S.S. Mansy, G. Gonzalez, M. Gilles-Gonzalez, M.K. Chan, Structure of a biological oxygen sensor: a new mechanism for heme-driven signal transduction, Proc. Natl. Acad. Sci. USA 95 (1998) 15177–15182.

[10] J.H.M. Cabral, A. Lee, S.L. Cohen, B.T. Chait, M. Li, R. Mackinnon, Crystal structure and functional analysis of the HERG potassium channel N terminus: a eukaryotic PAS domain, Cell 95 (1998) 649–655.

[11] S. Crosson, K. Moffat, Photoexcited structure of a plant photoreceptor domain reveals a light-driven molecular switch, Plant Cell 14 (2002) 1067–1075.

[12] T. Kinoshita, M. Doi, N. Suetsugu, T. Kagawa, M. Wada, K. Shimazaki, Phot1 and phot2 mediate blue light regulation of stomatal opening, Nature 414 (2001) 656–660.

[13] H. Kurokawa, D.S. Lee, M. Watanabe, I. Sagami, B. Mikami, C.S. Raman, T. Shimizu, A redox-controlled molecular switch revealed by the crystal structure of a bacterial heme PAS sensor, J. Biol. Chem. 279 (2004) 20186–201893.

[14] P.J. Erbel, P.B. Card, O. Karakuzu, R.K. Bruick, K.H. Gardner, Structural basis for PAS domain heterodimerization in the basic helix–loop–helix-PAS transcription factor hypoxia-inducible factor, Proc. Natl. Acad. Sci. USA 100 (2003) 15504–15509.

[15] J. Rutter, C.H. Michnoff, S.M. Harper, K.H. Gardner, S.L. McKnight, PAS kinase: an evolutionarily conserved PAS domain-regulated serine/threonine kinase, Proc. Natl. Acad. Sci. USA 98 (2001) 8991–8996.

[16] M. Procopio, A. Lahm, A. Tramontano, L. Bonati, D. Pitea, A model for recognition of polychlorinated dibenzo-*p*-dioxins by the aryl hydrocarbon receptor, Eur. J. Biochem. 269 (2002) 13–18.

[17] H.M. Berman, J. Westbrook, Z. Feng, G. Gilliland, T.N. Bhat, H. Weissig, I.N. Shindyalov, P.E. Bourne, The protein data bank, Nucleic Acids Res. 28 (2000) 235–242.

[18] B. Lee, F.M. Richards, Interaction of protein structures: estimation of static accessibility, J. Mol. Biol. 55 (1971) 379–400.

[19] S.I. Karchner, D.G. Franks, S.W. Kennedy, M.E. Hahn, The molecular basis for differential dioxin sensitivity in birds: role of the aryl hydrocarbon receptor, Proc. Natl. Acad. Sci. USA 103 (2006) 6252–6257.

Chemico-Biological Interactions 180 (2009) 238–244

Contents lists available at ScienceDirect

Chemico-Biological Interactions

journal homepage: www.elsevier.com/locate/chembioint

Structure-dependent activation of peroxisome proliferator-activated receptor (PPAR) γ by organotin compounds

Youhei Hiromori[a], Jun-ichi Nishikawa[b], Ichiro Yoshida[a], Hisamitsu Nagase[a], Tsuyoshi Nakanishi[a,c,*]

[a] Laboratory of Hygienic Chemistry and Molecular Toxicology, Gifu Pharmaceutical University, 5-6-1 Mitahora-higashi, Gifu, Gifu, 502-8585, Japan
[b] Laboratory of Health Sciences, School of Pharmacy and Pharmaceutical Sciences, Mukogawa Women's University, 11-68 Kyuban-cho, Koshien, Nishinomiya, Hyogo, 663-8179, Japan
[c] Department of Toxicology, Graduate School of Pharmaceutical Sciences, Osaka University, 1-6 Yamadaoka, Suita, Osaka, 565-0871, Japan

ARTICLE INFO

Article history:
Received 3 December 2008
Received in revised form 6 March 2009
Accepted 10 March 2009
Available online 24 March 2009

Keywords:
Butyltin
Phenyltin
Scatchard analysis
Tributyltin (TBT)
Triphenyltin (TPT)
Human chorionic gonadotropin (hCG)

ABSTRACT

Organotin compounds such as tributyltin (TBT) and triphenyltin (TPT) are frequent environmental contaminants and are suspected of disrupting endocrine function in vertebrates and invertebrates. Previously, we reported that TBT and TPT function as powerful agonists for peroxisome proliferator-activated receptor (PPAR) γ and stimulate adipocyte differentiation via the PPARγ signaling pathway. Our current study investigates the structure-dependent binding of butyltin and phenyltin compounds to PPARγ and their ability to activate the receptor. A Scatchard analysis with purified recombinant PPARγ demonstrated that [^{14}C]TPT binds to PPARγ with an equilibrium dissociation constant (K_d) of 66.6 ± 5.2 nM, which approximated the 46.2 ± 2.5 nM K_d of a typical PPARγ agonist, [^{3}H]rosiglitazone (Rosi). TBT, TPT, diphenyltin (DPT), and tetrabutyltin (TeBT) blocked the binding of [^{3}H]Rosi to PPARγ in a competitive manner, and all tested organotin compounds except monobutyltin blocked the binding of [^{14}C]TPT to PPARγ in a competitive manner. Unexpectedly, Rosi did not compete at all with [^{14}C]TPT for binding to PPARγ, and contrary to the results of the competition assay, TBT and TeBT, but not dibutyltin, transcriptionally activated a GAL–PPARγ chimeric receptor. All tested phenyltin compounds transcriptionally activated GAL–PPARγ with an order of potency of TPT > DPT > monophenyltin. In addition, treatment of human choriocarcinoma cells with TBT, TeBT, and all tested phenyltin compounds stimulated production of human chorionic gonadotropin, which is upregulated by PPARγ-mediated transcription. Our observations indicate that trialkylated and triphenylated tin compounds are the most potent PPARγ agonists among the alkylated and phenylated tin compounds, and a phenyl substituent on a tin atom enhances the potency of organotin compounds as a PPARγ agonist much more than a butyl substituent.

1. Introduction

Organotin compounds have been widely used as antifouling biocides for ships and fishing nets, agricultural fungicides, and rodent repellents [1,2]. These widespread uses have resulted in the release of increasing amounts of organotins into the environment. At very low concentrations, organotin compounds such as tributyltin (TBT) and triphenyltin (TPT) induce irreversible sexual abnormalities in female aquatic invertebrates, particularly marine gastropods, a condition termed "imposex" [3,4]. Organotins may also have various undesirable effects on human health [1,5]. It has been theorized that these compounds act in gastropods as potential competitive inhibitors of aromatase [3,6], which converts androgen to estrogen, resulting in increased levels of unconverted androgens, but their effective concentrations for aromatase inhibition are high [7–9]. In fact, at the same low concentrations needed to induce imposex, these compounds markedly enhance estradiol biosynthesis in human choriocarcinoma cells as well as increasing the activities of both aromatase [9] and 17β-hydroxysteroid dehydrogenase type I (17β-HSD I), which converts the low-activity estrogen estrone to the biologically more active form, estradiol [10]. Despite these reports describing the potential toxicity of organotins in vertebrates and invertebrates, the critical target molecules for the toxicity of organotin compounds remain unclear.

New insight into the mechanism of organotin toxicity is coming from a different direction. Recently, we identified TBT and TPT

Abbreviations: 17β-HSD I, 17β-hydroxysteroid dehydrogenase type I; 9cRA, 9-*cis*-retinoic acid; DBT, dibutyltin; DPT, diphenyltin; DMSO, dimethyl sulfoxide; FCS, fetal calf serum; GST, glutathione S-transferase; hCG, human chorionic gonadotropin; LUC, luciferase; MBT, monobutyltin; MPT, monophenyltin; PPAR, peroxisome proliferator-activated receptor; Rosi, rosiglitazone; PCR, polymerase chain reaction; RXR, retinoid X receptor; TBT, tributyltin; TeBT, tetrabutyltin; TePT, tetraphenyltin; TPT, triphenyltin.

* Corresponding author at: Laboratory of Hygienic Chemistry and Molecular Toxicology, Gifu Pharmaceutical University, 5-6-1 Mitahora-higashi, Gifu, 502-8585, Japan. Tel.: +81 58 237 3931; fax: +81 58 237 5979.
E-mail address: nakanishi@gifu-pu.ac.jp (T. Nakanishi).

0009-2797/$ – see front matter © 2009 Elsevier Ireland Ltd. All rights reserved.
doi:10.1016/j.cbi.2009.03.006

as nanomolar agonists for the retinoid X receptor (RXR), which is a member of the nuclear receptor superfamily [11–13]. Functional homologues of RXR have been cloned from Japanese and European gastropods (*Thais clavigera* and *Nucella lapillus*), and TBT binds to both of these homologs at environmentally relevant levels. Furthermore the natural ligand of RXR, 9-*cis*-retinoic acid (9cRA), induces imposex in both species of gastropods [11,14]. Organotin-induced estrogen biosynthesis in human choriocarcinoma cells, including mRNA expression of both aromatase and 17β-HSD I, also depends on the RXR signaling pathway [10,13]. These findings indicate that RXR activation is a critical event in the endocrine disruption caused by TBT and TPT in both gastropods and humans.

TBT and TPT also function as nanomolar agonists for the peroxisome proliferator-activated receptor (PPAR) γ, which is also a member of the nuclear receptor superfamily [12,15]. PPARγ regulates the expression of genes by heterodimerizing with RXR and by binding to the PPAR response elements in the target gene promoter [16,17]. PPARγ is activated by a variety of fatty acids and a class of synthetic antidiabetic agents, the thiazolidinediones [18]. PPARγ agonists such as rosiglitazone (Rosi) are used to treat type II diabetes and reverse insulin resistance in the whole body by sensitizing the muscle and liver tissue to insulin. PPARγ also serves as an essential regulator of adipocyte differentiation and lipid storage in mature adipocytes [19]. Unfortunately, the adipogenic activity of PPARγ may result in undesirable effects such as obesity. Indeed, we [12] and others [15] found that TBT and TPT stimulate adipocyte differentiation *in vitro* and *in vivo*, suggesting that organotin compounds are potential obesogens.

In addition, PPARγ is abundantly expressed in human trophoblast cells and serves as an essential regulator of placental differentiation and endocrine functions, including the production of human chorionic gonadotoropin (hCG) and steroidogenesis in human [20–22]. hCG is a luteotropic factor and stimulation by hCG governs not only progesterone production in the corpus luteum during the first trimester [23] but also testosterone production within the fetal testes [24]. Given the pivotal functional roles of hCG in sexual development and reproduction, factors that change PPARγ-mediated transcription in the placenta may greatly alter fetal development by disrupting these endocrine functions. Indeed, we found that some organotin compounds, including TBT and TPT, stimulate hCG production [9,13]. Activation of PPARγ by TBT and TPT represents a compelling mechanistic example of a class of environmental pollutants that have the ability to affect key adipogenic factors, fat deposit size, and placental functions.

Characterization of organotin compounds as RXR agonists has shown that binding of these organotin compounds to RXR and the responsiveness of the receptor depends on both the number and structure of the alkyl and aryl groups [13]. In addition, these observations suggest that the protein–ligand interactions between organotin compounds and RXR are very different from the interactions between 9cRA and synthetic retinoids [13]. To further our knowledge of how the toxicity of organotin compounds occurs via nuclear receptor signaling, we investigated the structure-dependent binding of butyltin and phenyltin compounds to PPARγ and their ability to activate the receptor. Furthermore, we investigated the correlation between their potency as agonists for PPARγ and hCG production in human choriocarcinoma cells.

2. Materials and methods

2.1. Chemicals

Tin compounds tested in this study were purchased from Tokyo Kasei Kougyo (Tokyo, Japan) or Aldrich Chemicals (Milwaukee, WI) and are listed in Table 1. Rosi was purchased from Cayman Chemical (Ann Arbor, MI). [^{3}H]Rosi (1.85 TBq/mmol) was purchased from American Radiolabeled Chemicals (Saint Louis, MO). [^{14}C]TPT (Tri[U-^{14}C]phenyltin hydroxide; radiochemical purity >96.6%, 2.04 GBq/mmol) was custom-made by Amersham Biosciences (Piscataway, NJ) [13]. All chemicals were dissolved in dimethyl sulfoxide (DMSO) (Nacalai Tesque, Kyoto, Japan). The standardized hCG was a kind gift from Asuka Pharmaceutical (Tokyo, Japan).

2.2. Cell cultures

Cells of the human choriocarcinoma cell line JEG-3 (ATCC No. HTB-36) and Jar (ATCC No. HTB-144) were obtained from ATCC (Manassas, VA). JEG-3 cells were cultured in minimal essential medium (MEM) with 2 mM L-glutamine, 0.1 mM MEM nonessential amino acid solution (Invitrogen, Carlsbad, CA), and 10% fetal calf serum (FCS). Jar cells were cultured in RPMI 1640 medium with 2 mM L-glutamine, 1 mM pyruvate, 4.5 g/L glucose, and 10% FCS. To determine the effect of organotin compounds on reporter gene expression and hCG secretion, the cells were seeded and precultured for 24 h and then treated with either organotin compounds in 0.1% DMSO or vehicle (0.1% DMSO) alone [9,13].

2.3. Plasmid construction

Full-length human PPARγ cDNA was amplified by reverse-transcriptase PCR using total RNA from JEG-3 cells and cloned into pGEX-2T (Amersham Biosciences). The sequences synthesized by PCR were confirmed by DNA sequencing. These constructs were used to generate glutathione S-transferase (GST)–PPARγ fusion proteins. The expression plasmid (pM-mPPAR1) for the ligand binding domain of mouse PPARγ fused to the DNA-binding domain of GAL4 (GAL–PPARγ) and the luciferase (LUC) reporter construct containing four copies of the GAL4 DNA binding site (UAS) followed by the thymidine kinase promoter (p4×UAS-tk-luc) used in the chimeric receptor assay were kind gifts from Dr. Y. Kamei (National Institute of Health and Nutrition, Japan) [12].

2.4. Ligand-binding assay

The GST–PPARγ fusions were expressed in *Escherichia coli* BL21 (DE3) cells and purified by using glutathione-Sepharose 4B (Amersham Biosciences). The purified proteins (30 μg/ml) were incubated with increasing concentrations of either [^{3}H]Rosi or [^{14}C]TPT with or without a 100-fold molar excess of each unlabeled compound. After incubation at 4 °C for 1 h, specific binding was determined with the hydroxyapatite binding assay, as described [13]. Binding in the presence of a 100-fold molar excess of unlabeled ligand was defined as nonspecific binding; specific binding was defined as total binding minus nonspecific binding. Similarly, butyltin and phenyltin compounds were used to compete for [^{3}H]Rosi and [^{14}C]TPT in this assay to determine the binding preferences of PPARγ.

2.5. Transient transfection assay

Transfection was performed with Lipofectamine reagent (Invitrogen) in accordance with the manufacturer's instructions. JEG-3 cells (3×10^4 cells) were seeded in 24-well plates 24 h before transfection with the optimal doses of the pM-mPPAR1 and p4×UAS-tk-luc DNA constructs. At 18 h after transfection, various compounds were added to the transfected cells, which were then cultured in regular culture medium supplemented with 1%

Table 1
Tin compounds tested in this study.

Tin compounds	Abbreviation	Purity (%)	CAS No.[a]	Maximal tested concentration[b]	Source
Butyltin trichloride (monobutyltin)	MBT	>95	1118-46-3	10 μM	Aldrich Chemicals
Dibutyltin dichloride	DBT	>97	683-18-1	100 nM	Tokyo Kasei Kougyo
Tributyltin chloride	TBT	>95	1416-22-0	100 nM	Tokyo Kasei Kougyo
Tetrabutyltin	TeBT	>93	1461-25-2	10 μM	Aldrich Chemicals
Phenyltin trichloride (monophenyltin)	MPT	>98	1124-19-2	10 μM	Aldrich Chemicals
Diphenyltin dichloride	DPT	>96	1135-99-5	1 μM	Aldrich Chemicals
Triphenyltin chloride	TPT	>95	639-58-7	100 nM	Aldrich Chemicals

[a] Chemical Abstracts Service registry number.
[b] Maximal tested concentrations of each tin compounds were defined as a maximal concentration at which the uptake of [3H]thymidine was ≥10% that for the vehicle alone (Ref. [10]).

charcoal-stripped FCS instead of 10% normal FCS. The cells were harvested 30 h later, and extracts were prepared and assayed for *firefly* LUC activity by using the dual-luciferase reporter assay system (Promega, Madison, WI) in accordance with the manufacturer's instructions. To normalize *firefly* LUC activity for transfection and harvesting efficiency, the *Renilla* LUC control reporter construct pRL-TK (Promega) was cotransfected as an internal standard in all reporter experiments. The results are expressed as the average relative *firefly* LUC activity of at least quadruplicate samples.

2.6. Determination of hCG production

hCG production was assessed as previously described [9,13]. In brief, Jar cells were seeded and treated with various compounds in regular culture medium supplemented with 5% charcoal-stripped FCS instead of 10% normal FCS for 48 h. To determine hCG production, the cells were washed and cultured in fresh medium for another 24 h. Culture supernatant was collected, and hCG concentration was determined by ELISA.

2.7. Statistics

All data from the control and treatment groups were obtained from the same numbers of replicated experiments. In addition, all the experiments were carried out independently 2 or 3 times. Dunnett's multiple comparisons test was applied to the raw data using SPSS 12.0J software (Chicago, IL). $P<0.05$ was taken as statistically significant.

3. Results

3.1. Scatchard analysis of [^{14}C]TPT binding to PPARγ

To directly characterize the binding affinities of butyltin and phenyltin compounds to PPARγ, we performed analyses of the saturation binding of [^{3}H]Rosi and [^{14}C]TPT to chimeric receptors, which consisted of GST fused to PPARγ (GST–PPARγ). Typical binding curves and Scatchard plots for [^{3}H]Rosi and [^{14}C]TPT binding to GST–PPARγ are shown in Fig. 1. The binding of both [^{3}H]Rosi and [^{14}C]TPT to GST–PPARγ was specific and saturating, and no binding was detected in control extracts from bacteria expressing GST (data not shown). Scatchard analyses of the binding of [^{3}H]Rosi to PPARγ yielded a K_d value of 46.2 ± 2.5 nM, which is similar to that previously reported [18], suggesting that this system is useful for determining the binding affinity of organotin compounds to PPARγ. Scatchard analyses of the binding of [^{14}C]TPT to PPARγ yielded a K_d value of 66.6 ± 5.2 nM. Although the K_d value of TPT for PPARγ was approximately 1.5-fold higher than that for Rosi, our results indicate that TPT binds to PPARγ with high affinity in a saturable and specific manner.

3.2. Competition of butyltin and phenyltin compounds with [^{3}H]Rosi and [^{14}C]TPT for binding to PPARγ

To further test which compounds might bind to PPARγ as ligands, we performed competitive ligand-binding assays. We measured the ability of [^{3}H]Rosi or [^{14}C]TPT to compete with the butyltin and phenyltin compounds for binding to GST–PPARγ. Consistent with our previous observations from a reporter gene assay [12], TBT and TPT competed with [^{3}H]Rosi for binding to PPARγ in a concentration-dependent manner (Fig. 2A and B). TPT was a more effective competitor for the binding of [^{3}H]Rosi to PPARγ than Rosi or TBT. In addition, diphenyltin (DPT) competed with [^{3}H]Rosi for binding to PPARγ as well as Rosi did (Fig. 2B). Tetrabutyltin (TeBT) also competed with [^{3}H]Rosi for binding to PPARγ, albeit approximately 10-fold less efficiently than Rosi. Dibutyltin (DBT) competed only slightly with [^{3}H]Rosi (Fig. 2A). Monobutyltin (MBT) and monophenyltin (MPT) failed to compete with [^{3}H]Rosi for binding to PPARγ (Fig. 2A and B).

TBT, TPT, and TeBT also successfully competed with [^{14}C]TPT for binding to PPARγ, and TPT was the most effective competitor among the tested compounds (Fig. 2C and D), consistent with the results of the competitive assay for [^{3}H]Rosi. MBT also failed to compete successfully with [^{14}C]TPT for binding. However, in contrast to the results of the competitive assay for [^{3}H]Rosi, DBT and MPT successfully competed for binding of [^{14}C]TPT (Fig. 2C and D). Unexpectedly, Rosi hardly competed with [^{14}C]TPT for binding. Although DPT competed with [^{14}C]TPT for binding when present at up to 30-fold excess, binding of [^{14}C]TPT increased in the presence of more than 100-fold excess of DPT (Fig. 2D). The high concentration of DPT may have promoted nonspecific binding of [^{14}C]TPT to GST–PPARγ, because same phenomenon was observed using GST instead of GST–PPARγ.

3.3. Activity of butyltin and phenyltin compounds as PPARγ agonists

To identify the functional potency of butyltin and phenyltin compounds as PPARγ agonists, we investigated the ability of butyltin and phenyltin compounds to activate PPARγ. We exposed JEG-3 cells to concentrations of organotins at which the uptake of [^{3}H]thymidine was ≥10% of that previously reported for the vehicle [10], and measured the responsiveness of the PPARγ receptor using a chimeric receptor consisting of the DNA-binding domain of the yeast transcription factor GAL4 and PPARγ (GAL–PPARγ) and a LUC reporter system. GAL–PPARγ binds to the GAL4 UAS in the promoter of the UAS-LUC reporter construct but can activate transcription only in the presence of the hybrid receptor's ligand. A particular advantage of the GAL4 receptor system is that the GAL4 hybrids provide a sensitive and effective means of assaying receptor–ligand interactions, even in the presence of the cells' endogenous wild-type receptors. Indeed, although PPARγ/RXR heterodimers can be fully activated by RXR agonists in addition to PPARγ agonists, we

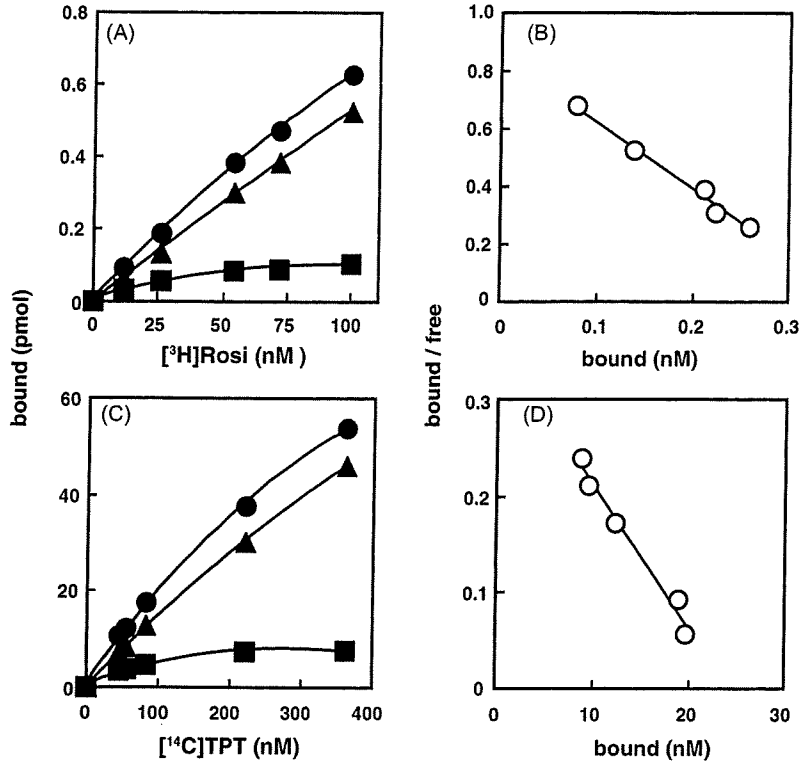

Fig. 1. Saturation binding and Scatchard analysis. (A and C) A GST–PPARγ fusion protein was incubated with increasing concentrations of [^{3}H]Rosi (A) or [^{14}C]TPT (C) in the absence or presence of a 100-fold molar excess of unlabeled Rosi (A) or TPT (C). Specific binding (closed squares) was defined as total binding (closed circles) minus nonspecific binding (closed triangles). (B and D) Scatchard analyses (open circles) were performed on specific binding data (duplicates at each point) for [^{3}H]Rosi (B) and [^{14}C]TPT (D) to yield the K_d values. Similar results were obtained in three independent experiments, and a representative experiment for each receptor–ligand combination is shown.

confirmed that 9cRA, which is a powerful agonist for RXR, failed to induce the expression of LUC in this system. Consistent with our previous observations, 100 nM TBT significantly induced the transactivation function of PPARγ (Fig. 3A, $P<0.01$), but the level of activation was less than that of Rosi. Although 10 μM TeBT also significantly activated transcription through GAL–PPARγ ($P<0.05$), the effective concentration was 100-fold higher and the level of activation was only slight compared with that induced by TBT and

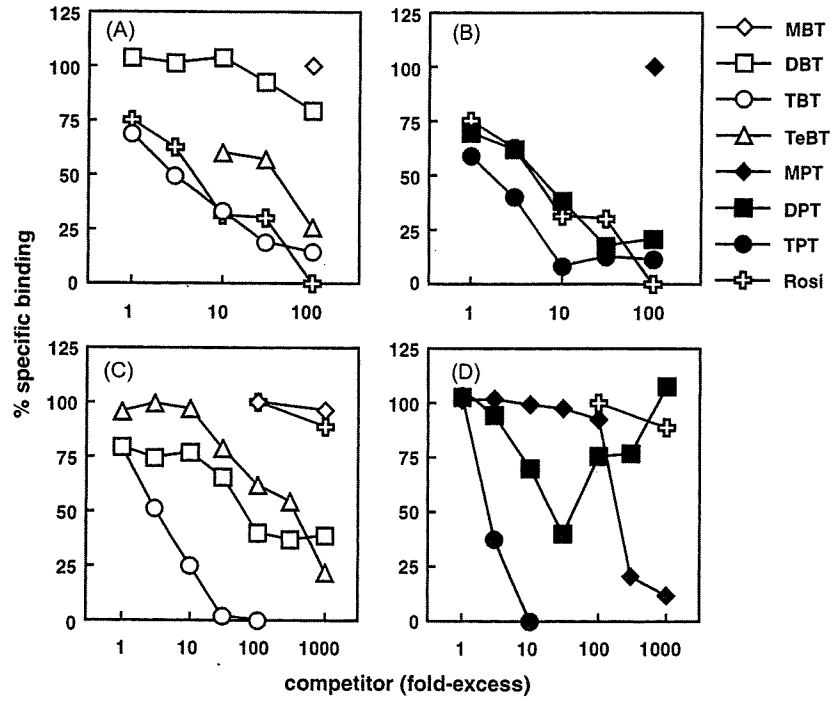

Fig. 2. Competition by Rosi and organotin compounds with [^{3}H]Rosi and [^{14}C]TPT for binding to PPARγ. A GST–PPARγ fusion protein was incubated with increasing concentrations of unlabeled Rosi and butyltins (A and C) or phenyltins (B and D) as competitors in the presence of 50 nM [^{3}H]Rosi (A and B) or 200 nM [^{14}C]TPT (C and D) as ligands. Each experiment was performed at least twice, and representative curves are shown.

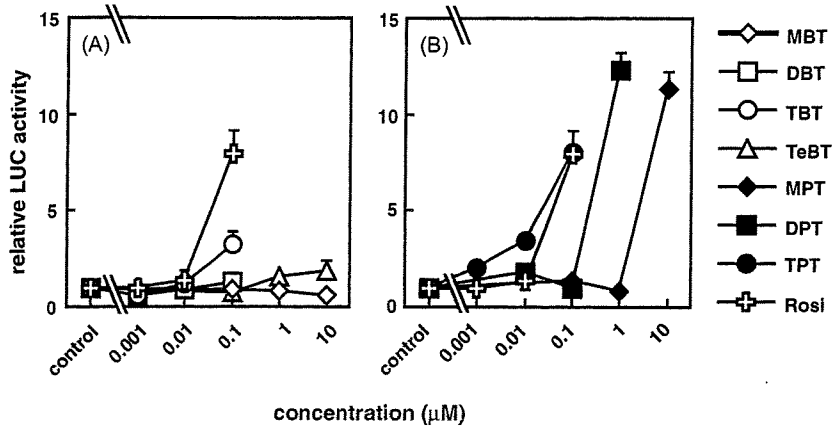

Fig. 3. Ability of organotin compounds to activate GAL–PPARγ. JEG-3 cells were cotransfected with 10 ng p4×UAS-tk-luc and 5 ng pM-mPPAR1 and then treated with Rosi and butyltins (A) or phenyltins (B). pRL-TK (2 ng) was cotransfected as the control for normalization of *Renilla* LUC activity (see Section 2). The results are expressed as average fold activation ± 1 S.D. after normalization to *Renilla* LUC activity.

Rosi (Fig. 3A). MBT and DBT induced no significant activation in the tested range (Fig. 3A).

In contrast, TPT significantly ($P<0.01$) induced the transactivation function of PPARγ at 1 nM, which is lower than the effective concentration of Rosi (Fig. 3B), suggesting that TPT is a more potential agonist for PPARγ than Rosi. In addition, both 10 μM MPT and 1 μM DPT significantly (both $P<0.01$) activated PPARγ at levels comparable to that of Rosi, but these concentrations are 100-fold and 10-fold higher, respectively, than the effective concentration of Rosi (Fig. 3B).

3.4. Production of hCG in Jar cells induced by butyltin and phenyltin compounds

We previously investigated the effects of all butyltin and phenyltin compounds tested in the current study on hCG production in human choriocarcinoma cells [9,13]. However, the tested concentrations in the previous study of these compounds, except for TBT and TPT, were too low to evaluate the correlation between their agonistic activity for PPARγ and hCG production. To investigate this correlation, we assessed the effects of these compounds on hCG production in Jar choriocarcinoma cells using the maximum concentrations tested in the experiment shown in Fig. 3. Consistent with our previous observations [9,13], 100 nM TBT and 100 nM TPT dramatically induced hCG production (Fig. 4), and the level of activation was much higher than that induced by Rosi (Fig. 4). hCG production was significantly induced by 10 μM MPT and 1 μM DPT at levels comparable to that of Rosi (Fig. 4). Although much less potent for the transactivation of PPARγ (Fig. 3A), 10 μM TeBT also induced hCG production at a level comparable to that of Rosi (Figs. 3 and 4). However, 10 μM MBT and 100 nM DBT failed to induce hCG production, in agreement with the results of the GAL–PPARγ transactivation assay (Figs. 3 and 4).

4. Discussion

We [11–13,25–27] and others [15] previously showed that TBT and TPT act as novel high-affinity xenobiotic agonists of RXR and PPARγ. This function of organotins was unexpected because the chemical composition and three-dimensional molecular structure of TBT and TPT are different from those of known natural and synthetic nuclear receptor ligands. The ability of tin compounds to bind to and activate RXR activity depends on both the number and length of their alkyl chains [13], but with the exception of a few butyltin compounds [15], the ability of organotins to bind to PPARγ and transactivate the receptor has not been investigated. We show here that the function of butyltin and phenyltin compounds as PPARγ agonists is structure-dependent, similar to their function as RXR agonists.

We first analyzed the K_d value of a typical endocrine-disrupting organotin, TPT, using a custom-made radiolabeled TPT. Our previous observations showed that the K_d values of TPT for RXRα, -β, and -γ were approximately 5–15-fold higher than those of 9cRA, the natural RXR agonist [13]. Here, the K_d value of TPT for PPARγ was comparable to that of Rosi, which is one of the highest-affinity thiazolidinediones [18], suggesting that TPT also binds to PPARγ with high affinity.

Next, we compared butyltins with phenyltins. In competition assays, both TBT and TPT competed with [^{3}H]Rosi and [^{14}C]TPT, but TPT was more competitive for both [^{3}H]Rosi and [^{14}C]TPT than TBT (Fig. 2). Consistent with these results, an approximately 10-fold lower concentration of TPT (10 nM) than of TBT (100 nM) was needed to elicit similar responses (Fig. 3). The di- and monosubstituted organotins DBT and MBT provided no significant activation, whereas DPT and MPT were moderately active in the micromolar range (Fig. 3). In addition, although MPT and MBT did not compete with [^{3}H]Rosi for binding to PPARγ, MPT, but not MBT, competed with [^{14}C]TPT, suggesting that MPT can bind to PPARγ. In our previous observations, both butyltins and phenyltins showed

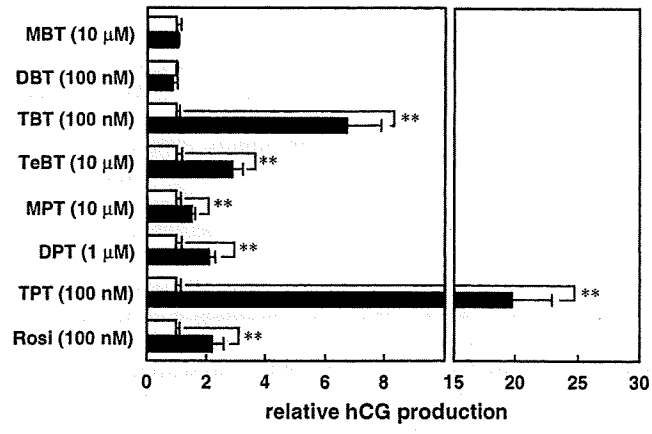

Fig. 4. Ability of organotin compounds to stimulate hCG secretion in Jar cells. Cells were treated with vehicle only (open bars) or the indicated compounds (filled bars) at the maximum concentrations tested in the experiment shown in Fig. 3. Results are expressed as mean ± 1 S.D. of triplicate cultures. The hCG production in vehicle-only cells, calculated from all experiments, was 290.0 ± 85.3 mIU/well/24 h. $^{**}P<0.01$.

similar potency for RXR [13], but our current results indicate that phenyltins are more potent for both binding and activating PPARγ than butyltins.

On the other hand, DBT competed with [^{14}C]TPT for binding to PPARγ better than MPT (Fig. 2C and D), although DBT failed to activate PPARγ at nanomolar concentrations (Fig. 3A) or at micromolar ranges (data not shown). These observations seem contradictory. However, the cytotoxicity of DBT is much greater than that of MPT because cells did not survive when treated with concentrations of DBT above 1 μM, but survived even when treated with 10 μM MPT [10]. In addition, the binding affinity of DBT for PPARγ is much less than that of TBT, although the cytotoxicity of DBT is greater than that of TBT [10]. Supporting this, we found that TBT was unable to activate PPARγ at concentrations above 500 nM because of its cytotoxicity (data not shown). Consequently, the cytotoxicity of DBT may render DBT-stimulated PPARγ activation undetectable.

The order of potency among the phenyltin compounds was TPT > DPT > MPT according to the results of both the competition and reporter gene assays (Figs. 2 and 3). Tetraphenyltin (TePT) was not tested in the current study because TePT does not dissolve well in DMSO or ethanol, and was therefore difficult to use in the current experiments. Instead, we used TeBT to investigate whether the presence of a fourth alkyl or aryl group would affect the potency as an agonist for PPARγ. Although TeBT significantly transactivated PPARγ, approximately 100-fold higher concentrations were needed than for TBT. In contrast, DBT had no activity for PPARγ (Fig. 3A). In addition, TeBT competed with [^{3}H]Rosi for binding to PPARγ, whereas DBT barely did (Fig. 2A). These results suggest that the presence of a fourth alkyl group on the tin atom decreases the potency of the organotin compounds for PPARγ, and, as with RXR [13], the order of potency is tri- > tetra- > di- > monosubstituted.

The hCG production induced by organotin compounds almost paralleled the results of GAL–PPARγ transactivation (Figs. 3 and 4). This was expected, because PPARγ agonists induce hCG production with a concomitant increase in mRNA expression [20,22]. However, the hCG production induced by 10 μM TeBT was comparable to that induced by 100 nM Rosi (Fig. 4), although TeBT had much lower ability to transactivate PPARγ (Fig. 3A). In addition, 100 nM TBT was more potent than 100 nM Rosi at inducing hCG production, although it was less potent in the transactivation of PPARγ (Figs. 3 and 4). Although these observations seem contradictory, RXR agonists as well as PPARγ agonists induce the production of hCG and mRNA expression of hCGβ (the subunit responsible for the biological specificity of hCG) [28–30] because hCG expression is upregulated by PPARγ/RXR heterodimers, which can be fully activated by ligands for either receptor and are activated synergistically in the presence of ligands for both. Our previous observation indicated that 100 nM TBT and 10 μM TeBT are enough to transactivate RXR [13]. Hence, TBT and TeBT may synergistically activate PPARγ/RXR heterodimers by acting as agonists for both receptors, leading to the induction of hCG production.

Although TPT functions as a high-affinity PPARγ agonist, Rosi did not compete with [^{14}C]TPT at all in our competition assay. Our observations suggest that the protein–ligand interaction between organotins and PPARγ may be markedly different from the interactions between Rosi and PPARγ. For example, in the PPARγ/RXR heterodimer, Rosi binds within the large PPARγ pocket in a U-shaped conformation, with the thiazolidinedione headgroup oriented toward the activation function 2 domain [31]. The thiazolidinedione headgroup makes hydrogen bonds with four residues of PPARγ (S289, H323, H449, and Y473). In contrast, TPT and other agonistic organotin compounds lack a thiazolidinedione headgroup, making their structures very different from that of the thiazolidinediones, such as Rosi. Although further studies are necessary to clarify which amino acids of PPARγ are important for the binding of organotin compounds to the ligand-binding pocket, the ligand–protein contacts of these compounds are most likely unique to each compound.

Human exposure to nonpoint sources of organotins occurs through contaminated dietary sources (seafood and shellfish), as fungicides on food crops, and as antifungal agents in wood treatments, industrial water systems, and textiles [32]. Measured exposure levels of butyltins and phenyltins in human tissue samples are in the range of 3–100 nM [32], high enough for TBT and TPT to activate PPARγ. PPARγ is the target for antidiabetic drugs, but also serves as an essential regulator of adipocyte differentiation and lipid storage in mature adipocytes [19]. Although TBT is suspected to be an environmental obesogen that acts via PPARγ signaling [15], TPT is as prevalent in the environment as TBT but has higher potency and is therefore likely to present an even bigger public health problem.

To our knowledge, this is the first study to characterize butyltin and phenyltin compounds as PPARγ agonists. Our results indicate that the potency of organotin compounds for PPARγ is structure-dependent and that phenyltin compounds are more potent agonists than butyltin compounds. Although many reports have described the potential toxicity of organotins, it remains unclear whether this toxicity involves PPARγ signaling. Therefore, future studies are needed to investigate the precise mechanisms, including PPARγ signaling, underlying the toxicity induced by organotin compounds to distinguish the toxic effects of organotins from similar adverse effects, such as cardiac hypertrophy, edema, hemotoxicity, and hepatotoxicity, that have been associated with existing antidiabetic PPARγ agonists in animal models or in humans [33,34].

Conflict of interest

None declared.

Acknowledgments

This research was supported in part by grants from the Industrial Technology Research Grant Program in 2007 from NEDO (New Energy and Industrial Technology Development Organization of Japan); the Environmental Technology Development Fund of the Ministry of the Environment of Japan (FY2008); and a Grant-in-Aid for Scientific Research from the Ministry of Education, Science, Sports, and Culture of Japan. We thank Dr. Y. Kamei (National Institute of Health and Nutrition, Japan) for providing the plasmids pM-mPPAR1 and p4×UAS-tk-luc, and Asuka Pharmaceutical (Tokyo, Japan) for providing the standardized hCG for the ELISA.

References

[1] I.J. Boyer, Toxicity of dibutyltin, tributyltin and other organotin compounds to humans and to experimental animals, Toxicology 55 (3) (1989) 253–298.
[2] K. Fent, Ecotoxicology of organotin compounds, Crit. Rev. Toxicol. 26 (1) (1996) 1–117.
[3] P. Matthiessen, P.E. Gibbs, Critical appraisal of the evidence for tributyltin-mediated endocrine disruption in mollusks, Environ. Toxicol. Chem. 17 (1) (1998) 37–43.
[4] T. Horiguchi, H. Shiraishi, M. Shimizu, M. Morita, Effects of triphenyltin chloride and five other organotin compounds on the development of imposex in the rock shell, *Thais clavigera*, Environ. Pollut. 95 (1) (1997) 85–91.
[5] T.J. Benya, Bis(tributyltin) oxide toxicology, Drug Metab. Rev. 29 (4) (1997) 1189–1284.
[6] C. Bettin, J. Oehlmann, E. Stroben, TBT-induced imposex in marine neogastropods is mediated by an increasing androgen level, Helgol. Meeresunters. 50 (1996) 299–317.
[7] G.M. Cooke, Effect of organotins on human aromatase activity in vitro, Toxicol. Lett. 126 (2) (2002) 121–130.
[8] D.D. Heidrich, S. Steckelbroeck, D. Klingmuller, Inhibition of human cytochrome P450 aromatase activity by butyltins, Steroids 66 (10) (2001) 763–769.
[9] T. Nakanishi, J. Kohroki, S. Suzuki, J. Ishizaki, Y. Hiromori, S. Takasuga, N. Itoh, Y. Watanabe, N. Utoguchi, K. Tanaka, Trialkyltin compounds enhance human CG secretion and aromatase activity in human placental choriocarcinoma cells, J. Clin. Endocrinol. Metab. 87 (6) (2002) 2830–2837.

[10] T. Nakanishi, Y. Hiromori, H. Yokoyama, M. Koyanagi, N. Itoh, J. Nishikawa, K. Tanaka, Organotin compounds enhance 17β-hydroxysteroid dehydrogenase type I activity in human choriocarcinoma JAr cells: potential promotion of 17β-estradiol biosynthesis in human placenta, Biochem. Pharmacol. 71 (9) (2006) 1349–1357.
[11] J. Nishikawa, S. Mamiya, T. Kanayama, T. Nishikawa, F. Shiraishi, T. Horiguchi, Involvement of the retinoid X receptor in the development of imposex caused by organotins in gastropods, Environ. Sci. Technol. 38 (23) (2004) 6271–6276.
[12] T. Kanayama, N. Kobayashi, S. Mamiya, T. Nakanishi, J. Nishikawa, Organotin compounds promote adipocyte differentiation as agonists of the peroxisome proliferator-activated receptor γ/retinoid X receptor pathway, Mol. Pharmacol. 67 (3) (2005) 766–774.
[13] T. Nakanishi, J. Nishikawa, Y. Hiromori, H. Yokoyama, M. Koyanagi, S. Takasuga, J. Ishizaki, M. Watanabe, S. Isa, N. Utoguchi, N. Itoh, Y. Kohno, T. Nishihara, K. Tanaka, Trialkyltin compounds bind retinoid X receptor to alter human placental endocrine functions, Mol. Endocrinol. 19 (10) (2005) 2502–2516.
[14] L.F. Castro, D. Lima, A. Machado, C. Melo, Y. Hiromori, J. Nishikawa, T. Nakanishi, M.A. Reis-Henriques, M.M. Santos, Imposex induction is mediated through the retinoid X receptor signalling pathway in the neogastropod *Nucella lapillus*, Aquat. Toxicol. 85 (1) (2007) 57–66.
[15] F. Grun, H. Watanabe, Z. Zamanian, L. Maeda, K. Arima, R. Cubacha, D.M. Gardiner, J. Kanno, T. Iguchi, B. Blumberg, Endocrine-disrupting organotin compounds are potent inducers of adipogenesis in vertebrates, Mol. Endocrinol. 20 (9) (2006) 2141–2155.
[16] S.A. Kliewer, K. Umesono, D.J. Noonan, R.A. Heyman, R.M. Evans, Convergence of 9-*cis* retinoic acid and peroxisome proliferator signalling pathways through heterodimer formation of their receptors, Nature 358 (6389) (1992) 771–774.
[17] I. Issemann, R.A. Prince, J.D. Tugwood, S. Green, The peroxisome proliferator-activated receptor: retinoid X receptor heterodimer is activated by fatty acids and fibrate hypolipidaemic drugs, J. Mol. Endocrinol. 11 (1) (1993) 37–47.
[18] J.M. Lehmann, L.B. Moore, T.A. Smith-Oliver, W.O. Wilkison, T.M. Willson, S.A. Kliewer, An antidiabetic thiazolidinedione is a high affinity ligand for peroxisome proliferator-activated receptor γ (PPARγ), J. Biol. Chem. 270 (22) (1995) 12953–12956.
[19] P. Tontonoz, E. Hu, B.M. Spiegelman, Stimulation of adipogenesis in fibroblasts by PPARγ2, a lipid-activated transcription factor, Cell 79 (7) (1994) 1147–1156.
[20] W.T. Schaiff, M.G. Carlson, S.D. Smith, R. Levy, D.M. Nelson, Y. Sadovsky, Peroxisome proliferator-activated receptor γ modulates differentiation of human trophoblast in a ligand-specific manner, J. Clin. Endocrinol. Metab. 85 (10) (2000) 3874–3881.
[21] T. Fournier, L. Pavan, A. Tarrade, K. Schoonjans, J. Auwerx, C. Rochette-Egly, D. Evain-Brion, The role of PPARγ/RXRα heterodimers in the regulation of human trophoblast invasion, Ann. N.Y. Acad. Sci. 973 (2002) 26–30.
[22] A. Tarrade, K. Schoonjans, J. Guibourdenche, J.M. Bidart, M. Vidaud, J. Auwerx, C. Rochette-Egly, D. Evain-Brion, PPARγ/RXRα heterodimers are involved in human CGβ synthesis and human trophoblast differentiation, Endocrinology 142 (10) (2001) 4504–4514.
[23] T. Yoshimi, C.A. Strott, J.R. Marshall, M.B. Lipsett, Corpus luteum function in early pregnancy, J. Clin. Endocrinol. Metab. 29 (2) (1969) 225–230.
[24] I.T. Huhtaniemi, C.C. Korenbrot, R.B. Jaffe, HCG binding and stimulation of testosterone biosynthesis in the human fetal testis, J. Clin. Endocrinol. Metab. 44 (5) (1977) 963–967.
[25] T. Nakanishi, J. Nishikawa, K. Tanaka, Molecular targets of organotin compounds in endocrine disruption: do organotin compounds function as aromatase inhibitors in mammals? Environ. Sci. 13 (2) (2006) 89–100.
[26] T. Nakanishi, Potential toxicity of organotin compounds via nuclear receptor signaling in mammals, J. Health Sci. 53 (1) (2007) 1–9.
[27] T. Nakanishi, Endocrine disruption induced by organotin compounds: organotins function as a powerful agonist for nuclear receptors rather than an aromatase inhibitor, J. Toxicol. Sci. 33 (3) (2008) 269–276.
[28] J. Guibourdenche, E. Alsat, F. Soncin, C. Rochette-Egly, D. Evain-Brion, Retinoid receptors expression in human term placenta: involvement of RXRα in retinoid induced-hCG secretion, J. Clin. Endocrinol. Metab. 83 (4) (1998) 1384–1387.
[29] J. Guibourdenche, S. Roulier, C. Rochette-Egly, D. Evain-Brion, High retinoid X receptor expression in JEG-3 choriocarcinoma cells: involvement in cell function modulation by retinoids, J. Cell Physiol. 176 (3) (1998) 595–601.
[30] A. Tarrade, C. Rochette-Egly, J. Guibourdenche, D. Evain-Brion, The expression of nuclear retinoid receptors in human implantation, Placenta 21 (7) (2000) 703–710.
[31] R.T. Gampe Jr., V.G. Montana, M.H. Lambert, A.B. Miller, R.K. Bledsoe, M.V. Milburn, S.A. Kliewer, T.M. Willson, H.E. Xu, Asymmetry in the PPARγ/RXRα crystal structure reveals the molecular basis of heterodimerization among nuclear receptors, Mol. Cell 5 (3) (2000) 545–555.
[32] B. Antizar-Ladislao, Environmental levels, toxicity and human exposure to tributyltin (TBT)-contaminated marine environment—a review, Environ. Int. 34 (2) (2008) 292–308 b_antizar@hotmail.com.
[33] V. Sood, K. Colleran, M.R. Burge, Thiazolidinediones: a comparative review of approved uses, Diabetes Technol. Ther. 2 (3) (2000) 429–440.
[34] H.E. Lebovitz, Differentiating members of the thiazolidinedione class: a focus on safety, Diabetes Metab. Res. Rev. 18 (Suppl. 2) (2002) S23–29.

Environ. Sci. Technol. 2009, 43, 6611–6616

Identification of Retinoic Acid Receptor Agonists in Sewage Treatment Plants

HUAJUN ZHEN,[†] XIAOQIN WU,[†] JIANYING HU,*[,†] YANG XIAO,[†] MIN YANG,[†] JUNJI HIROTSUJI,[§] JUN-ICHI NISHIKAWA,[∥] TSUYOSHI NAKANISHI,[⊥] AND MICHIHIKO IKE[#]

Laboratory for Earth Surface Processes, College of Urban and Environmental Sciences, Peking University, Beijing 100871, China, State Key Lab of Environmental Aquatic Chemistry, Research Center for Eco-Environmental Sciences, Chinese Academy of Sciences, Beijing 100085, China, Advanced Technology R&D Center, Mitsubishi Electric Co., 8-1-1 Tsukaguchi-Honmachi, Amagasaki, Hyogo 661-8661, Japan, Department of Pharmacology, Faculty of Pharmaceutical Sciences, Mukogawa Women's University, 11-68 Koshien Kyubancho, Nishinomiya City, Japan, Laboratory of Hygienics, Gifu Pharmaceutical University, 5-6-1 Mitahora-higashi, Gifu 502-8585, Japan, and Division of Sustainable Energy and Environmental Engineering, Graduate School of Engineering, Osaka University, 2-1 Yamadaoka, Suita, Osaka 565-0871, Japan

Received July 12, 2008. Revised manuscript received July 13, 2009. Accepted July 19, 2009.

Retinoic acid receptor (RAR) agonists are speculated to be one possible cause for the widely observed frog deformities in North America, although little is known about the specific RAR agonists in aquatic environments. We identified the specific RAR agonists in sewage treatment plants (STPs) and receiving rivers using an RAR yeast two-hybrid bioassay. Water samples were extracted by solid-phase extract cartridges, which were successively eluted by hexane, ethyl acetate, and methanol for bioassay. Among the three fractions, the ethyl acetate fraction showed the highest RAR agonistic activities. The bioassay-derived activity, expressed as all-*trans*-retinoic acid (all-*trans*-RA) equivalents (ATRA-EQ) were 10.9 ± 2.2 and 1.7 ± 1.0 ng/L in the STP influents and effluents, respectively, while the ATRA-EQs were as high as 7.1 and 8.3 ng/L in the two rivers receiving STP effluents. Following a two-step fractionation using high-performance liquid chromatography and ultra-performance liquid chromatography (UPLC) directed by the bioassay, two bioactive fractions were obtained from Gaobeidian STP influent and all-*trans*-4-oxo-RA (4.7–10.4 ng/L in influents, <0.2–0.9 ng/L in effluents) and 13-*cis*-4-oxo-RA (2.3–7.1 ng/L in influents, <0.4–1.1 ng/L in effluents) were identified in these fractions with UPLC-MS/MS. The EC_{50} for all-*trans*-4-oxo-RA or 13-*cis*-4-oxo-RA relative to that of all-*trans*-RA in exhibiting RARα agonistic activity was calculated to be 3.87 and 0.46, respectively.

Introduction

A number of papers have highlighted the potentially detrimental effects of naturally occurring and man-made chemicals on reproductive and developmental processes in wildlife and humans (*1*–*4*). Previous studies have paid special attention to some endocrine-disrupting chemicals which exert estrogenic activity via binding to the estrogen receptor (ER), through which the ligand–receptor complex subsequently activates transcription of target genes (*5*–*7*). There exist a number of nuclear hormone receptors such as the ER, androgen receptor (AR), thyroid receptor (TR), retinoic acid receptor (RAR), and vitamin D receptor (VDR), which mediate the actions of hormones and vitamins to affect processes from reproduction to development and even general metabolism (*8*). Thus, environmental pollutants binding to a wide variety of nuclear hormone receptors could induce adverse effects in wildlife (*9*), as exemplified by a recent study that organotins caused imposex in gastropods through the involvement of retinoid X receptors (RXRs) (*10*).

As one of these nuclear hormone receptors, RARs, which include three subtypes α, β, and γ, are raising the concern of environmental scientists. RARs control aspects of vision, cell differentiation, immune response, and also embryonic development in vertebrates (*11*). Ligands of RARs have been reported to be potential teratogens in developing embryos, and an agonist specific for each subtype exhibits different teratogenic patterns. RARα ligand causes deformity in the ear and mandible, and causes limb malformations, while RARβ agonist induces malformations in the liver and urinary system, and the ligand for RARγ causes ossification deficiencies and defects of the sternabrae and vertebral bodies (*12*). The natural ligands for RARs are endogenous retinoic acids (RAs) derived from retinoid (vitamin A) precursors (*13*). An excess or a deficiency of RA and related retinoids can cause abnormal morphological development, which was proven to be an RAR-mediated process (*12*). It was found that treating the larvae of Japanese flounder (*Paralichthys olivaceus*) with RA would cause deformities in the lower jaw, caudal fin, and vertebrae (*14*). Previous studies with *Xenopus laevis* have shown that exposure to RA or the RA precursor, retinyl palmitate, would induce malformations in eyes and hindlimbs (*15*–*18*), and similar phenomena including eye abnormalities, extra/missing limbs and/or digits have also been observed in wild frogs (*19*–*22*). Accordingly, the presence of RAR agonists was suggested to be one possible cause for the increasing trend of wildlife malformation (*18, 23*).

The natural RAs, which are derived from retinoid (vitamin A) precursors in humans and animals have three isomers (all-*trans*-RA, 9-*cis*-RA, and 13-*cis*-RA), and all-*trans*-RA and 13-*cis*-RA are also used in clinical treatment of dermatosis (*24*) and in cancer prevention and chemotherapy (*25*). Besides RAs, many endogenous compounds have been reported to be agonists of RARs. Some RA metabolites in humans and animals such as 4-oxo-RA, 4-hydroxy-RA, 18-hydroxy-RA, and 5,6-epoxy-RA can also bind to RARs (*26, 27*). These chemicals could be present in the environment by domestic sewage discharging and medical usage. More recently, a large number of synthetic compounds have also been proven to show RAR agonistic activity in vitro, such as organochlorine pesticides, styrene dimers, monoalkylphenols, and parabens (*28*–*30*). To date, few studies have investigated the occurrence

* Corresponding author phone and fax: 86-10-62765520; e-mail: hujy@urban.pku.edu.cn.
† Peking University.
‡ Chinese Academy of Sciences.
§ Mitsubishi Electric Co.
∥ Mukogawa Women's University.
⊥ Gifu Pharmaceutical University.
Osaka University.

10.1021/es9000328 CCC: $40.75
Published on Web 07/29/2009

of potential RAR agonists in aquatic environments (*23*, *31*). In a study from Canada, Alsop et al. found that methanol and dichloromethane extracts from three pulp mill effluents were able to displace more than 25% of the [^{3}H]all-*trans*-RA which bound to RARs from white sucker (*Catostomus commersoni*) gills (*31*). Gardiner et al. tested two water samples collected from Minnesota and California ponds and lakes where malformed frogs were frequently discovered, and a high response of RARα agonistic activity was detected in water samples from both places (*23*). To the best of our knowledge, however, the causative chemicals have not been identified and no paper has reported the occurrence of RAR agonistic activity in STP effluents and their receiving waters.

In this study, we determined the RAR agonistic activity in seven sewage treatment plants and their receiving rivers in Beijing, China using the RARα yeast two-hybrid bioassay. Then we identified two causative chemicals applying bioassay-directed HPLC fractionation followed by LC-MS/MS analysis.

Materials and Methods

Sample Collection. By using flow-proportional samplers, 24-h composite samples of the influents and effluents were collected each day during a one-week period (June 26 to July 2, 2006) from seven sewage treatment plants (STPs) in Beijing, China. These STPs are all operated with primary and secondary treatment processes without any post disinfection or additional filtration step. All of the plants mainly receive domestic wastewater, and detailed information on the STPs and sampling dates are summarized in Table S1 (Supporting Information). We also collected water samples by single time-point sampling from the Tonghui River and Qing River (their widths are between 15 and 25 m), which receive the effluents from Gaobeidian and Qinghe STP, respectively, in the summer (July 2, 2006) and winter (January 2, 2007). In the Tonghui River, we found two wastewater discharging pipes located at 0.55 and 2.6 km downstream, which contributed to the water flow in the Tonghui River as well as Gaobeidian STP effluent. Therefore, we set the sampling sites along the Tonghui River at 2 km upstream, and 0.5, 0.55, 2.55, and 2.6 km downstream from the discharge point of Gaobeidian STP. The sampling sites for the Qing River were located at 4 and 2 km upstream, and 2 and 4 km downstream, of the Qinghe STP. All samples were filtered and extracted within 6 h after collection. In addition, 300 mL of human urine was collected from a healthy volunteer, and a 100 mL fresh swine serum sample was purchased from National Hyclone Bio-Engineering (Lanzhou, China). Additional information about sample collection is provided in the Supporting Information.

Sample Preparation and Solid Phase Extraction (SPE) Fractionation. Water samples were filtered with a 1.2-μm pore size Whatman GF/C glass fiber pad (Maidstone, UK). After filtration, the pH of the samples was adjusted to 3.0 by adding hydrochloric acid. Oasis HLB cartridges (6 mL, Waters, USA) were conditioned by a sequence of 6 mL of hexane, 6 mL of ethyl acetate, 6 mL of methanol, and 12 mL of ultrapure water at a flow rate of 5−10 mL/min. Then 250 mL of influents, 500 mL of effluents, and 2 L of river water were extracted by passing them through 200 mg, 200 mg, and 500 mg cartridges under vacuum at a flow rate of 5−10 mL/min, respectively. The cartridges were rinsed with 10 mL of ultrapure water, and then dried under a flow of nitrogen. The dried cartridges were eluted by a sequence of 6 mL of hexane (F1), 6 mL of ethyl acetate (F2), and 6 mL of methanol (F3), respectively. The detailed sample preparation procedure is shown in Figure S1. For the influent and effluent samples, 7-day eluents of each fraction were pooled as composite samples for a complete week. Thus, 1.75 L of influent and 3.5 L of effluent from each STP were finally concentrated to 1.75 and 0.7 mL for individual fractions, respectively. Mixed eluents were prepared by combining 100 μL of each fraction to reach 300 μL in total volume. As for river water, the 2 L sample was concentrated to 400 μL for each fraction, and 100 μL of each fraction was combined to get 300 μL of mixed eluent. To determine the RAR agonistic activity of STP and river water samples, each fraction (100 μL) and the mixed sample (300 μL) were first concentrated under a gentle stream of nitrogen at room temperature, and then redissolved in 100 μL of DMSO. Finally, the concentration factors for the yeast assay of influents, effluents, and river water were 1000, 5000, and 5000, respectively. Experimental blanks were taken by extracting 2 L of ultrapure water using the same method as described above, and none of them were detected to exhibit RAR agonistic activities. The urine sample was treated using the same procedure as the water samples, and the serum sample was prepared as described in a previous study (*32*).

Two-Step Reversed-Phase Fractionation Using HPLC and UPLC. For the SPE fraction that showed RAR agonistic activity in the bioassay, a further reversed-phase HPLC fractionation was conducted. Separation was accomplished by a 4.6 mm × 250 mm symmetry shield RP18 column (Waters, Massachusetts). The column was maintained at room temperature at a flow rate of 1 mL/min. Solvent A was ultrapure water, and solvent B was acetonitrile. The gradient was started at 20% B, and was held for 3 min (0−3 min). Then the gradient was brought to 100% B in 27 min (3−30 min), and held for 10 min (30−40 min). Finally, the gradient was brought down to 20% B in 0.1 min, and this percentage was kept for 10 min (40−50 min) until the next injection. The UV detector was set at double wavelengths of 254 and 350 nm. As shown in Figure S1, 1.55 mL F2 fractions of influents, 0.5 mL F2 fractions of effluents, and 0.2 mL F2 fractions of river water samples by SPE from the seven STPs and two rivers were first concentrated under a flow of nitrogen and then fractionated by HPLC. The discrete fractions by HPLC were collected at 2-min intervals. Half of each collection was freeze-dried for yeast assay, and the other half of each collection was preserved for UPLC/MS/MS analysis. The freeze-dried collections were redissolved in 77.5 μL and 50 μL DMSO for the influent and effluent, respectively, and therefore the final concentration factors of influent and effluent were 10,000 and 25,000 for the yeast assay. For UPLC-MS/MS analysis, the collections were concentrated under a flow of nitrogen and redissolved in 60% acetonitrile solution. The final volumes for influents, effluents, and river water were 100, 100, and 50 μL, which made concentration factors of 7750, 12,500, and 10,000 for influents, effluents, and river water, respectively. The information of chemicals, UPLC-ESI-MS/MS condition, and quantitation and quality assurance/quality control (QA/QC) are provided in the Supporting Information.

For the HPLC fraction that showed RAR agonistic activity in the bioassay, ACQUITY ultra-performance liquid chromatography (Waters, Milford, MA) with great improvement of chromatographic resolution was further used for fractionation. Separation was accomplished by a Waters ACQUITY UPLC BEH C18 column (100 mm × 2.1 mm, 1.7 μm particle size). The column was maintained at 30 °C at a flow rate of 0.2 mL/min. Solvent A was 0.1% formic acid in ultrapure water, and solvent B was acetonitrile. The isocratic condition with 60% B was used for chromatographic separation. Fifty μL of the HPLC F15 fraction for influent from Gaobeidian STP, which represents 500 mL of influent, was fractionated by UPLC (Figure S1). The discrete fractions were collected at 0.5-min intervals. The collections were first freeze-dried, and then redissolved in 50 μL of DMSO for yeast assay at a concentration factor of 10,000.

Yeast Assay for RAR-mediated Activity. The yeast two-hybrid assay described in a previous paper (*33*) was applied

to evaluate the RAR-mediated activity of samples, and a detailed description is provided in the Supporting Information.

According to the guide for the derivation and application of relative potency estimates from in vitro bioassay data, multiple-point based estimates would be reasonable to characterize the potency of a variety of samples in in vitro bioassay (*34*). However, in this study, the responses for most of the STP influent and effluent samples and river water samples were less than 20% of the maximal response of all-*trans*-RA in bioassay. Thus, we evaluated the relative potency of samples and calculated the all-*trans*-RA equivalents (ATRA-EQs) based on a single-point estimation using nonlinear regression according to the dose–response curve of all-*trans*-RA developed on the same day (*34*).

Results and Discussion

RARα Agonistic Activity in Sewage Treatment Plants. Wastewater samples were extracted and eluted in three fractions, F1, F2 and F3, which represented the nonpolar, medium polar, and polar substances in the samples, and a mixed sample was reconstituted from the three fractions. The RARα agonistic activity was characterized by comparing the response magnitude caused by samples to the maximum induction by all-*trans*-RA standard at 100 nmol/L.

Of the three fractions, the F2 fraction exhibited the greatest RARα agonistic activity in both influents and effluents from all seven STP samples. In the STP influents, the magnitudes of the responses for F2 fractions ranged from 6.1% (Jiuxianqiao STP) to 21.9% (Gaobeidian STP) all-*trans*-RA Max at a concentration factor of 1000. For the effluent samples, the F2 fractions exhibited magnitudes of responses from 3.6% (Xiaohongmen STP) to 24% (Fangzhuang STP) all-*trans*-RA Max at a concentration factor of 5000. The ATRA-EQ in the F2 fractions ranged from 6.6 ng/L (Jiuxianqiao STP) to 13.4 ng/L (Wujiacun STP), and 0.9 ng/L (Jiuxianqiao STP) to 3.2 ng/L (Fangzhuang STP) for the influent and effluent samples (Table S2), respectively, which indicated that the current treatment processes can effectively remove the RARα agonists in the F2 fractions of wastewater. Among all the effluents and influents from the seven STPs, only two F1 fractions of influents exhibited weak RARα agonistic activity (Figure 1). The F1 fraction mainly contained nonpolar compounds. As for the F3 fractions, no significant RARα agonistic activities were observed in any of the samples.

For the mixed samples of three fractions, only one of the seven STP influents showed weak RARα agonistic activity, while three of the seven STP effluents exhibited relatively strong RARα agonistic activities (Figure 1). Since all F2 fractions were observed to exhibit RARα agonistic activities, this phenomenon would be explained by the presence of the matrix. Thus, the mixed samples of three fractions were spiked by 50 μg/L all-trans-RA, and the inhibition was estimated (Supporting Information) to be up to 86–103% in the influents of Fangzhuang, Beixiaohe, Jiuxianqiao, and Qinghe STPs and about 67% in the effluents except for Fangzhuang STP (97%).

RARα Agonistic Activity in Receiving River Waters. To investigate the occurrence of RAR agonists in river water due to the discharge of STP effluents, we collected water samples from the Tonghui River and Qing River, which received the effluents from Gaobeidian STP and Qinghe STP, respectively. The water samples were taken in the summer (July 2006) and winter (January 2007) from upstream and downstream of the STP discharging sites.

Similar to the results for the samples from the STPs, significant RARα agonistic activities in river water samples were observed in the F2 fractions from both the Tonghui River and Qing River (Figure 2), and their corresponding ATRA-EQ values are listed in Tables S3 and S4. It should be

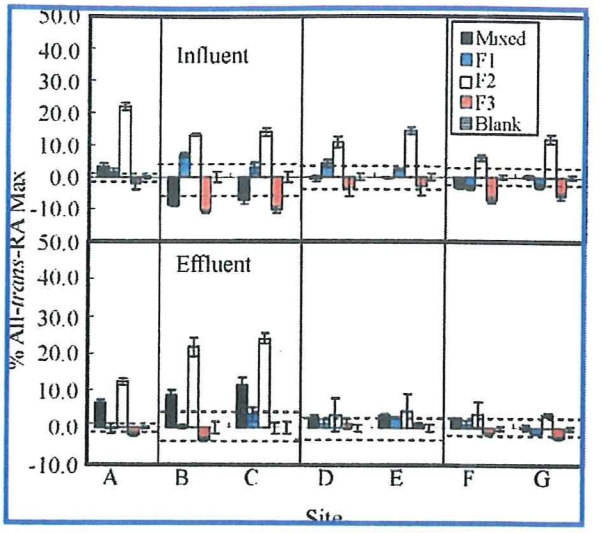

FIGURE 1. RARα agonistic activity of the influents (upper panels) and effluents (lower panels) in the seven Beijing sewage treatment plants during summer 2006. The concentration factors for influent and effluent are 1000 and 5000, respectively. Response magnitude stands for the percentage of the average maximum response observed for a 100 nmol/L all-*trans*-RA standard (% All-*trans*-RA Max). Dashed lines represent ±3 standard derivation (SD) from the mean solvent control response (set to 0% All-*trans*-RA Max): A Gaobeidian; B Beixiaohe; C Fangzhuang; D Xiaohongmen; E Wujiacun; F Jiuxianqiao; G Qinghe.

noted that two samples taken from downstream Tonghui River (0.55 and 2.6 km downstream) in both the summer and winter exhibited unexpectedly high responses of RARα agonistic activities, even higher than the activities in the corresponding STP effluents, indicating that there were other input sources in both rivers. In a previous paper reporting on the occurrence of natural and synthetic glucocorticoids at the same sites in the Tonghui River, it was also found that the concentrations of glucocorticoids were unexpectedly higher than those in the corresponding STP effluent samples (*35*). These elevated concentrations are most likely caused by a wastewater discharging pipe at the 0.55 km site (Pipe 1) which contributed greatly to the total load of glucocorticoids in downstream river. Thus, we collected the wastewater (in January 2007) from Pipe 1 (0.55 km downstream) and Pipe 2 (2.6 km downstream), and found that the F2 fractions of the samples from Pipes 1 and 2 exhibited much higher RARα agonistic activities than the river water at 0.55 and 2.6 km downstream, respectively. The ATRA-EQ in the two samples from Pipes 1 and 2 were calculated to be 67 and 94 ng/L, which were 9.4 and 11.3 times those of samples taken from the corresponding river sites, 7.1 and 8.3 ng/L, respectively (Table S3). As for the sample taken from upstream Tonghui River (2 km upstream), the RARα agonistic activities in F2 fractions were slightly higher than those from Gaobeidian STP effluents in both the summer and winter, which might be due to the undiscovered discharging sources along the upstream Tonghui River.

On the other hand, two samples from upstream (4 and 2 km upstream) of the Qing River in both summer and winter exhibited unexpectedly high responses of RARα agonistic activities. Such distribution along the Qing River is different from that of natural and synthetic glucocorticoids at the same sites in the Qing River (*35*). Considering that the glucocorticoids are originally from the discharge of humans and animals, the unexpectedly high RARα agonistic activities might be due to the discharge of other unknown sources, which needs further investigation. It is interesting that the